

AD-765 479

DEVELOPMENT OF AN AIR-DRIVEN ALTERNATOR
FOR 60-MM MORTAR APPLICATION-PHASE II

Carl J. Campagnuolo, et al

Harry Diamond Laboratories
Washington, D. C.

May 1973

DISTRIBUTED BY:

NTIS

National Technical Information Service
U. S. DEPARTMENT OF COMMERCE
5285 Port Royal Road, Springfield Va. 22151

AD

AD 765479

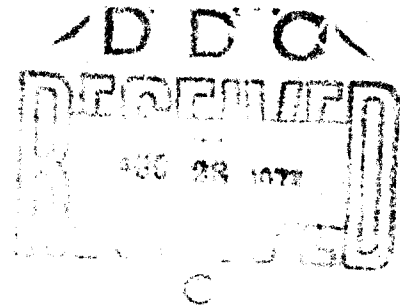
HDL-TM-73-7

DEVELOPMENT OF AN AIR-DRIVEN ALTERNATOR
FOR 60-mm MORTAR APPLICATION-PHASE II

C.J. Campagnuolo

J.E. Fine

May 1973



U.S. ARMY MATERIEL COMMAND

HARRY DIAMOND LABORATORIES

WASHINGTON, D.C. 20438

APPROVED FOR PUBLIC RELEASE, DISTRIBUTION UNLIMITED

UNCLASSIFIED

Security Classification

DOCUMENT CONTROL DATA - R & D

(Security classification of title, body of abstract and indexing annotation must be entered when the overall report is classified)

1. ORIGINATING ACTIVITY (Corporate author)		2a. REPORT SECURITY CLASSIFICATION	
Harry Diamond Laboratories Washington, D. C. 20438		UNCLASSIFIED	
		2b. GROUP	
3. REPORT TITLE			
DEVELOPMENT OF AN AIR-DRIVEN ALTERNATOR FOR 60-mm MORTAR APPLICATION - PHASE II			
4. DESCRIPTIVE NOTES (Type of report and inclusive dates)			
5. AUTHOR(S) (First name, middle initial, last name)			
Carl J. Campagnuolo and Jonathan E. Fine			
6. REPORT DATE		7a. TOTAL NO. OF PAGES	7b. NO. OF REFS
May 1973		56	2
8a. CONTRACT OR GRANT NO.		8b. ORIGINATOR'S REPORT NUMBER(S)	
a. PROJECT NO DA-1W564602D02815		HDL-TM-73-7	
c. AMCMS Code: 664602.12.24715		8b. OTHER REPORT NO'S (Any other numbers that may be assigned this report)	
d. HDL Proj. No. 442234			
10. DISTRIBUTION STATEMENT			
Approved for public release; distribution unlimited.			
11. SUPPLEMENTARY NOTES		12. SPONSORING MILITARY ACTIVITY	
		U.S. Army Materiel Command	
13. ABSTRACT			
<p>An air-driven alternator that was developed to provide electrical energy and a second safing signature for the 60-mm Multioption Fuze for mortars (MOFM) was tested successfully in the wind tunnel, in a rain field, and in extreme temperature environment conditions.</p> <p>The alternator design was modified so that it can be fabricated from low-cost stamped parts in large quantities. The new design satisfies the electrical power requirements of the fuze.</p>			

DD FORM 1473

1 NOV 65

REPL. CES DD FORM 1473, 1 JAN 64, WHICH IS
OBSOLETE FOR ARMY USE.

UNCLASSIFIED

Security Classification

55

Security Classification

UNCLASSIFIED

Security Classification

AD

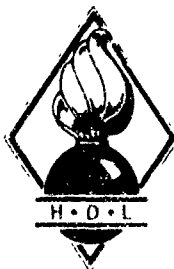
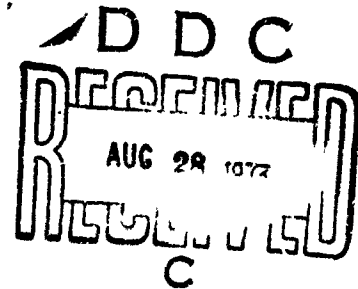
DA-1W564602D02815
AMCMS Code: 664602.12.24715
HDL Proj. No. 442234

HDL-TM-73-7

**DEVELOPMENT OF AN AIR-DRIVEN ALTERNATOR
FOR 60-mm MORTAR APPLICATION-PHASE II**

**C.J. Campagnuolo
J.E. Fine**

May 1973



U.S. ARMY MATERIEL COMMAND
HARRY DIAMOND LABORATORIES
WASHINGTON DC 20438

APPROVED FOR PUBLIC RELEASE, DISTRIBUTION UNLIMITED

ACKNOWLEDGEMENT

The authors wish to acknowledge the assistance and contributions made by the other members of the HDL Mortar Fuze Staff.

We wish to express special thanks to Mr. G. Scillian for his suggestions in the development of the alternator design.

ABSTRACT

An air-driven alternator that was developed to provide electrical energy and a second safing signature for the 60-mm Multioption Fuze for mortars (MCFM) was tested successfully in the wind tunnel, in a rain field, and in extreme temperature environment conditions.

The alternator design was modified so that it can be fabricated from low-cost stamped parts in large quantities. The new design satisfies the electrical power requirements of the fuze.

TABLE OF CONTENTS

<u>Section</u>	<u>Title</u>	<u>Page</u>
	ABSTRACT	3
1	INTRODUCTION	9
2	FUZE POWER REQUIREMENTS	11
3	SUMMARY OF PREVIOUS STUDIES OF THE 500 SERIES ALTERNATOR	12
4	RAIN TEST ON ALTERNATOR	16
	4.1 Introduction	16
	4.2 Test Hardware	16
	4.3 Tests	16
	4.4 Results	19
5	TEMPERATURE TESTS OF 60 mm ROTARY POWER SUPPLY FROM -60° TO +160° F	22
	5.1 Purpose	22
	5.2 Experimental Apparatus and Procedure	22
6	WIND TUNNEL TEST OF ALTERNATOR PERFORMANCE . . .	34
	6.1 Introduction	34
	6.2 Description of Test	34
	6.3 Wind Tunnel Test Results	40
7	DEVELOPMENT OF 600 SERIES ALTERNATOR	45
	7.1 Stator Design	45
	7.2 Magnet Rotor Design	45
	7.3 Tests With Alnico 6	45
8	SUMMARY	51
9	CONCLUSIONS	51
	DISTRIBUTION LIST	53

Preceding page blank

LIST OF ILLUSTRATIONS

<u>Figure</u>	<u>Title</u>	<u>Page</u>
1	500 series alternator components and assembly.	10
2	Operating range of 60-mm power supply.	13
3	Voltage, current, and power supplied to fuze electrical circuit by 60-mm power supply	14
4	Telemetered performance of HDL design power supply during flight of 60-mm mortar	15
5	Sled mounted on track prior to high-speed run.	17
6	Voltage-reducing circuit	18
7	High-velocity run in rain field for alternator No. 6.	20
8	Low-velocity run in rain field for alternator No. 6.	21
9	High-velocity run in rain field for alternator No. 7.	23
10	Low-velocity run in rain field for alternator No. 7.	24
11	High-velocity run in rain field for alternator No. 8.	25
12	Low-velocity run in rain field for alternator No. 8.	26
13	High-velocity run in rain field for alternator No. 9.	27
14	Low-velocity run in rain field for alternator No. 9.	28
15	Alternator mounted in temperature test chamber.	30
16	Instrumentation for temperature test of alternator.	31
17	Experimental arrangement for studying effect of temperature on alternator output	32
18	Power output versus velocity for three values of inlet gas temperature	35
19	Apparatus for measuring alternator rotation speed vs velocity in wind tunnel	36
20	HDL fuze ogive	37
21	ABCA fuze ogive	38
22	Laboratory test arrangement	40
23	Alternator rotational speed in laboratory and in wind tunnel - HDL fuze ogive	41
24	Alternator rotational speed in laboratory and in wind tunnel - ABCA ogive	42
25	Rotational speed vs angle of attack at mach numbers of 0.20, 0.30, 0.39, and 0.63 for HDL fuze ogive	43
26	Rotational speed vs angle of attack at mach numbers of 0.20, 0.30, 0.39, and 0.63 for ABCA fuze ogive.	44
27	600 series alternator components and assembly	45
28	Electrical power vs velocity for various stator pole widths	47
29	Electrical power vs velocity for rotors with different lengths	48

LIST OF ILLUSTRATIONS (Continued)

<u>Figure</u>	<u>Title</u>	<u>Page</u>
30	Electrical power output and rotational speed of 600 series alternator over 60-mm velocity range	49
31	High power output obtainable from 600 series casings at subsonic velocity	50

LIST OF TABLES

<u>Table</u>	<u>Title</u>	<u>Page</u>
I	Laboratory comparison of alternator output before and after rain test	29

1. INTRODUCTION

The design objectives for the Multioption Fuze for mortars (MOFM), to be used on projectiles for the lightweight 60-mm mortar, contained the requirements for an electrical power supply that would furnish adequate power even when fired at zero-charge increment, as well as for dual signatures for safing and arming in accordance with MIL-STD-1316A. To meet these requirements, an air-driven alternator was designed to power the fuze and to mechanically drive the safing and arming system (S&A) into the armed position during flight. The first arming signature can be obtained at launch from the acceleration setback forces. A second arming signature is provided by the operation of the alternator only during projectile flight. The alternator did meet the requirement for providing adequate electrical power for the fuze when the 60-mm projectile was fired at zero-charge increment.

The air-driven alternator (fig. 1) converts in-flight ram-air energy into the electrical energy required by the fuze. During flight, air enters through an intake at the projectile nose and is directed to a turbine wheel. The kinetic energy of the air is converted by the turbine to mechanical-rotational energy; the exhaust air is then expelled through holes uniformly spaced around the circumference of the fuze ogive. The rotational motion of the wheel is then transferred to a cylindrical permanent magnet rotor by a concentric shaft. The rotor turns between the poles of a magnetic stator and induces an emf in the armature windings.

The concentric shaft extends through the rotor to a speed reducer. The output of the speed reducer rotates the safing and arming device from a safe out-of-line position to the armed in-line position.

Alternators, similar to the type described herein, were used on proximity fuzes for bombs, rockets, and mortars during World War II. The primary reason was that reserve power supplies, such as those used in high-spin artillery applications, could not be used effectively in low-spin environments. Development of a thermal reserve power supply eliminated the need for alternators.

The enactment of MIL-STD-1316A, wherein dual safing signatures are required, virtually excludes all existing mortar fuze systems if pull pins, etc., are excluded as a second safety signature. This new requirement created interest in alternator power supplies for mortar applications, because both safety and electric power could be derived from a single component.

The initial development of the turbine-driven alternator, designated as "500 Series," has been reported.¹ This report describes the performance of the device as well as preliminary environmental and field tests. This report, a continuation of this work, contains results of tests such as rain tests, exposure

¹Campagnuolo, Carl J. and Jonathan E. Fine, "Development of the HDL Air-Driven Rotary Generator to Power a 60 mm Fuze," Harry Diamond Laboratories, TM-72-2, Washington D.C., Mar 1972

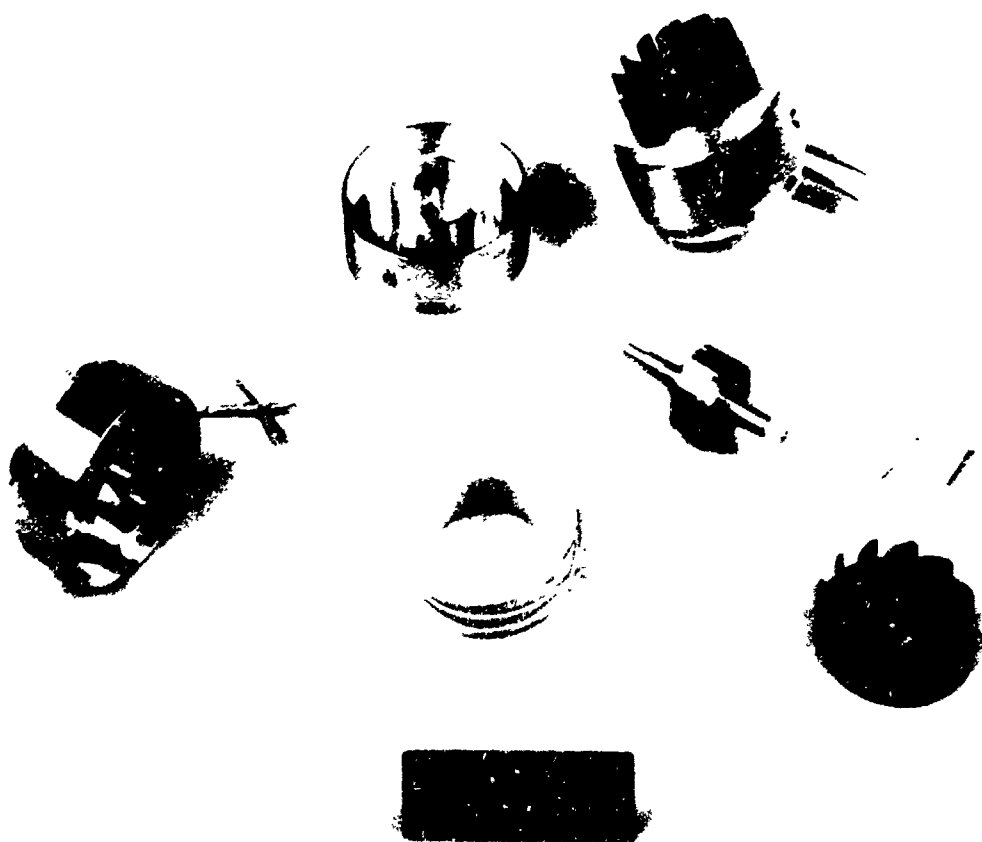


Figure 1. 500 series alternator components and assembly.

to temperature extremes, and wind tunnel tests conducted on the 500 series design. In addition, the development of a small alternator (600 series) is discussed. This second alternator is similar in design to the 500 series, and can be manufactured at lower cost by using high-production techniques. Hence, all the results of environmental tests conducted with the 500 series will also be valid for the 600 series alternator.

2. FUZE POWER REQUIREMENTS

The operating range of the power supply is established by the flight trajectory of the projectile which leaves the muzzle with a characteristic velocity and travels in a parabolic arc. Because of the effect of gravity and air drag, the projectile velocity decreases during the ascent phase of the flight to a minimum value at the apex of the arc and then increases during descent, attaining a terminal velocity approximately equal to the muzzle velocity. For large elevations (85 deg), the speed at the apex is about 10 percent of the muzzle velocity.

For this reason, the portion of the trajectory over which the power supply is required to function must be specified. For the concept-feasibility design it was necessary to demonstrate that the generator produced the required power when fired at the lowest charge, and that it could initiate during descent when fired at the steepest angle of elevation (85 deg). Hence, the turbine must start at a threshold velocity of about 120 ft/sec or lower, so that the generator can provide power to the fuzing system.

The generator must supply electrical power to the fuzing circuit and also provide a mechanical output from the generator shaft to the safing and arming (S&A) system. For the mechanical output, the spinning shaft drives a gear-reduction system that aligns the firing pin with the detonator at a specified safe distance from the gun.

The requirements for the power supply are:

1. It must generate 0.600W with a 600- Ω load at flight velocities varying from 150 ft/sec to about 850 ft/sec.
2. It must fit into a space no greater than 1 cu in.
3. It must retain its integrity when spinning at velocities greater than 100,000 rpm for at least 40 sec.
4. It must be simple to manufacture and to assemble.
5. If the alternator stops during the low-velocity phase of the flight, it must restart during the high-velocity phase in time to power a fuze.
6. The fuze drag must not adversely affect the range and stability of the round.

7. The alternator must have a long storage life and be rugged enough to withstand the gun environment.

8. It must not be adversely affected by flight through rain.

The studies reported here were conducted on the alternator alone. A later report will describe the effect of the safing and arming system on the performance of the alternator.

3. SUMMARY OF PREVIOUS STUDIES OF THE 500 SERIES ALTERNATOR

The development of the design for the 500 series alternators has been reported by these authors (ref 1). Some of the salient results from this reference are summarized below.

Figure 2 shows the electrical power and rotational speed as a function of velocity over the anticipated flight range of the mortar. The alternator generates 0.6 W in a 600- Ω load at 150 ft/sec and produces a maximum of 1.2 W at the higher velocities. The rotational speed increases with velocity and reaches a maximum of 180,000 rpm at 850 ft/sec. However, when the alternator shaft is connected to the safing and arming system, the rotational speed will be considerably reduced. Figure 3 gives the voltage and the current produced when the alternator supplies a simulated fuze electrical circuit. The fuze requires 14 to 17 volts to operate. The alternator produces 16 volts at 125 ft/sec inlet velocity.

Several alternators were fired at charge zero from the 60-mm mortar at 45 degrees quadrant elevation. The frequency and rectified output voltage of the alternators were monitored during the flight by means of telemetry. The telemetered voltage supplied to the fuze circuit is plotted in figure 4 as a function of time into flight for two of the rounds.

In the first round, a rectified output of 25 Vdc was supplied after the projectile left the muzzle. Then the voltage decreased and reached a minimum of 15 volts near the apex of the trajectory. The voltage then increased during descent and reached a level of 27 Vdc before impact. Note that because of the inertia of the alternator rotor, the rotational speed and output voltage that occurs immediately after the round leaves the gun is lower than that at corresponding velocity near termination of the trajectory. As indicated in figure 4, the 500 series alternator design can power the fuze during the entire flight of the round.

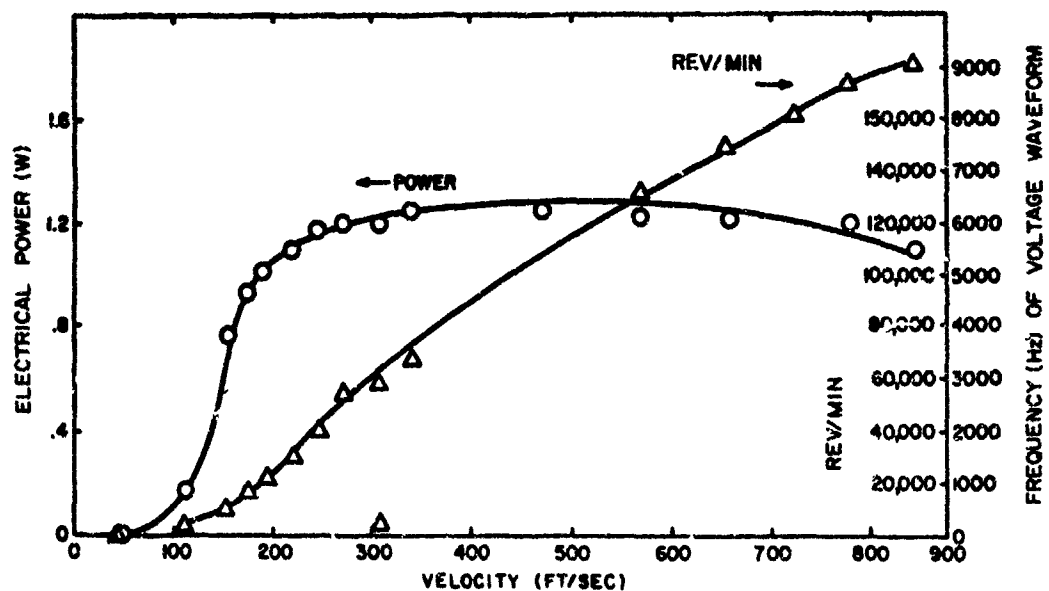


Figure 2. Operating range of 60-mm power supply.

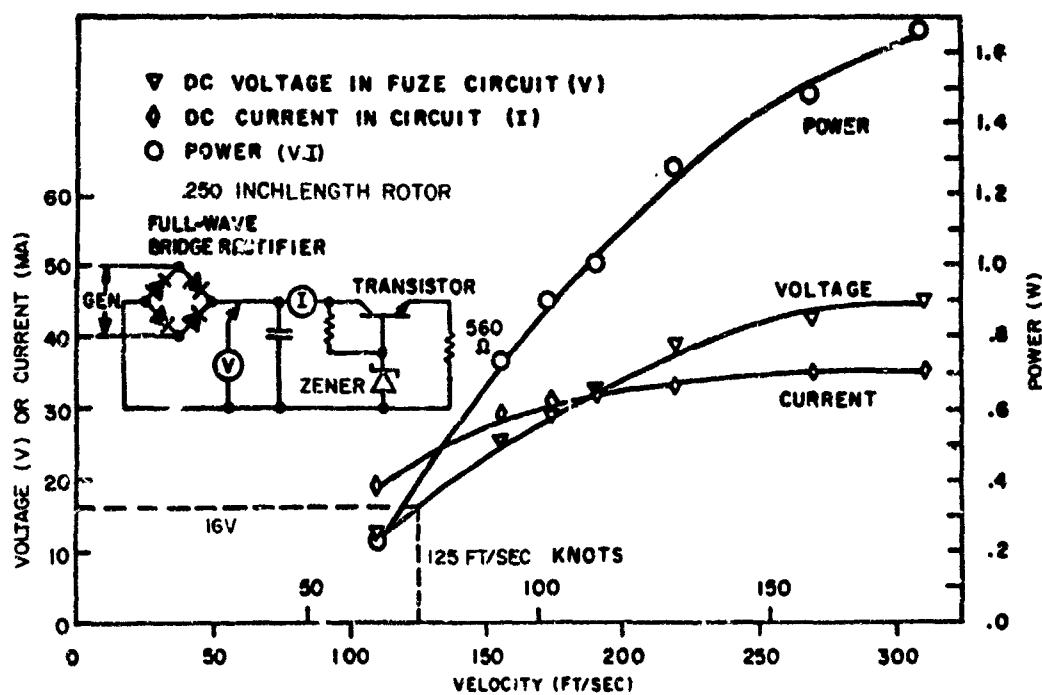


Figure 3. Voltage, current, and power supplied to fuze electrical circuit by 60-mm power supply.

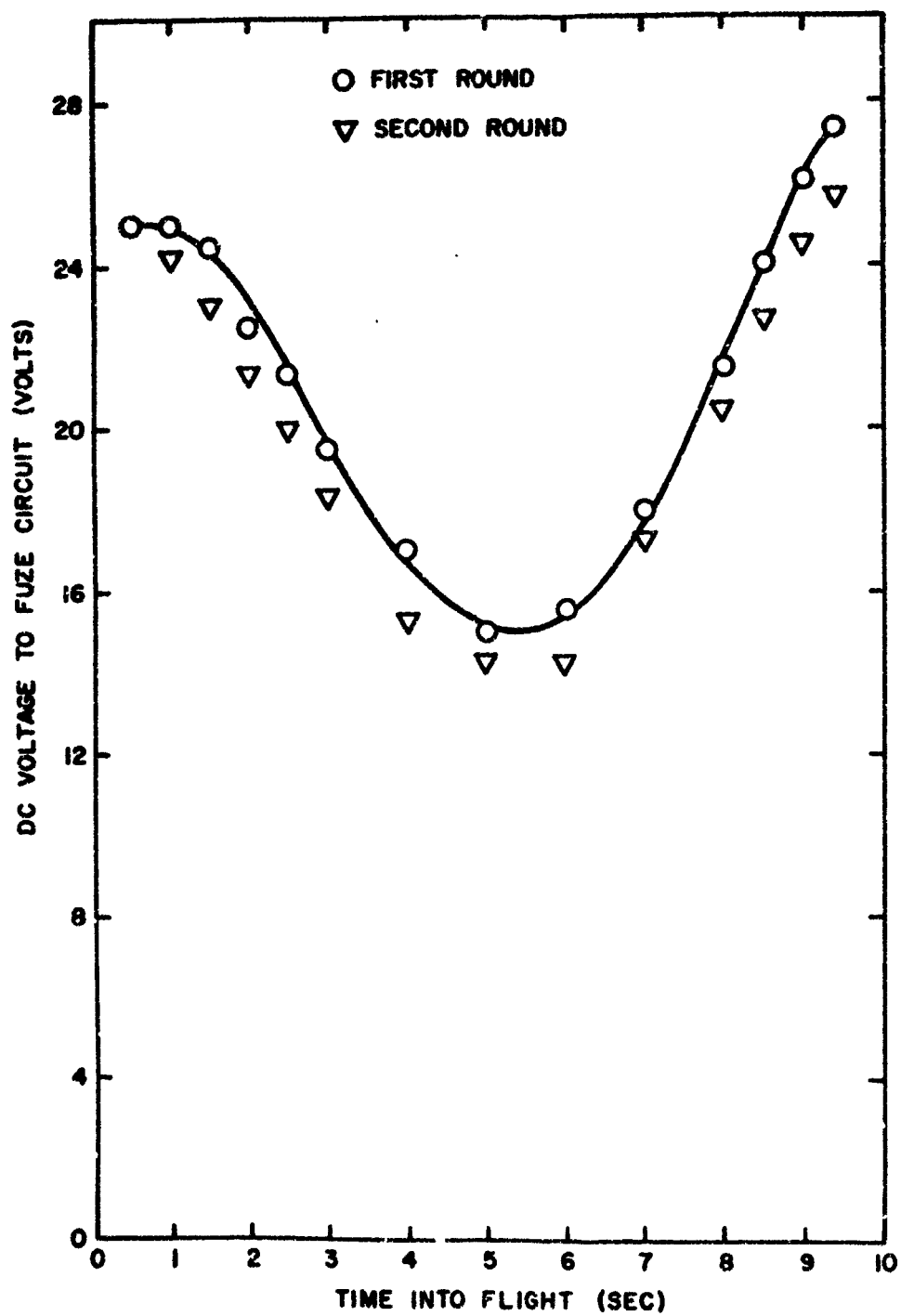


Figure 4. Telemetered performance of HDL design power supply during flight of 60-mm mortar.

4. RAIN TEST ON ALTERNATOR

4.1 Introduction

Two tests were conducted at Holloman Air Force Base with the 500 series alternator to determine the functioning characteristics of the alternators under simulated rain conditions of 24 in. hr.² The alternators were mounted on a sled propelled by rocket motors through a rain field 2000 ft in length (fig. 5). The voltage output of each device was monitored via telemetry. In the first tests, the sled accelerated from zero velocity, entered the rain field at a velocity of 650 ft/sec, and left the rain field 3.83 sec later at a velocity of 410 ft/sec. In the second test, the sled entered the rain field at a velocity of 430 ft/sec and left at a velocity of 250 ft/sec 6.18 sec later. The two runs together provided data from 10.0 sec in the rain field over the velocity range from 250 to 650 ft/sec.

4.2 Test Hardware

For the rain test, each alternator was housed in a fuze ogive having an entrance port 0.380 in. in diameter and rectangular exit ports (0.500 in. x 0.130 in.) uniformly spaced around the circumference. The entrance and exit ports were completely open to simulate firing from a mortar.

To monitor the alternator output during the sled run, a special circuit was designed that would reduce the rectified alternator output by a factor of 20 and supply 0 to 7 V dc, the voltage limit of the telemetry system. The circuit is shown in figure 6.

All alternators were mounted in fuze ogives and tested in the laboratory. Pressures corresponding to the flight velocity expected in a sled were supplied to the alternators and the output voltage was recorded. The alternators were also checked when mounted on the sled, to ensure that the telemetry recording equipment was operating properly. Laboratory tests were conducted after the device had flown in the rain to determine any damage to the alternator parts from passage through the rain field.

4.3 Tests

The Holloman test track is 37,000 ft long, and the rain-field section of the track extends over some 2000 ft. Rain was simulated by forcing water through a series of nozzles on both sides of the track. The entry and exit points of the sled in the rain field were located 25,032 and 23,032 ft from the end of the track, respectively. Weather stations, located in the rain section of the track at intervals of approximately 1000 ft, provided information about wind speed and direction. The velocity of the sled during the test was measured every 200 ft along the full length of the track. The telemetered output of the alternators was recorded at a ground station on oscillograph charts and on magnetic tapes. The time of entry and time of exit of the sled from the rain field was marked on the oscillograph charts and magnetic tapes.

²Balogh, Nicholas, "Fluid Generator Rain Tests Runs 43R-A1 and 43R-B1," Final Report Project 921C, Holloman AFB, N.M., 26 May 1972.



Figure 5. Sled mounted on track prior to high-speed run.

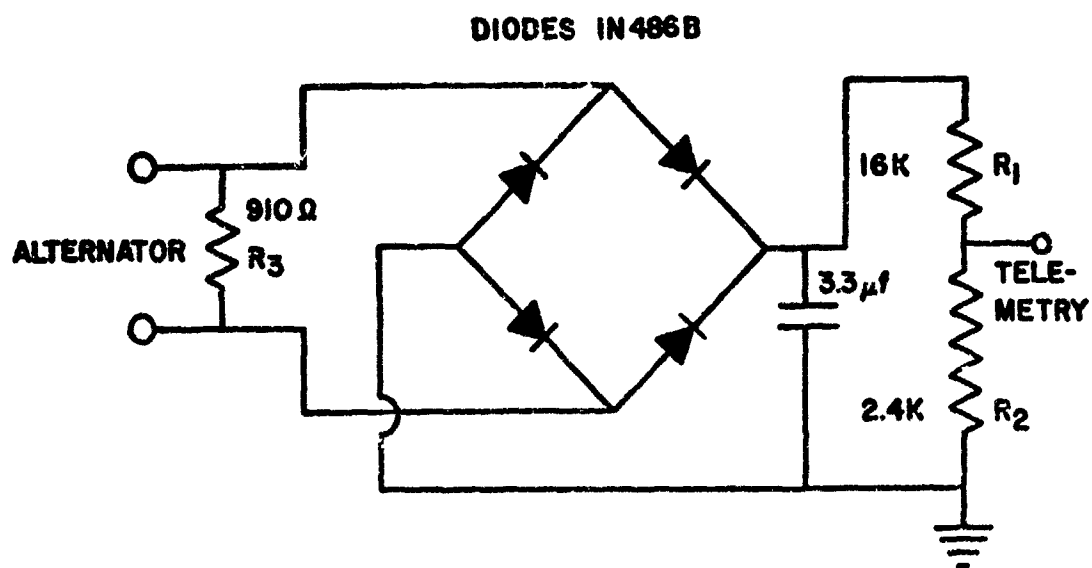


Figure 6. Voltage-reducing circuit.

The prime objective of the test was to obtain data in the rain field from 200 to 800 ft/sec, the proposed velocity profile of the 60-mm mortar. Because the 2000-ft-rain field length did not permit the entire velocity profile to be performed on a single run, two runs were conducted. The sled was programmed to enter the rainfield at 800 ft/sec and exit at 450 ft/sec during the first test. For the second run, the sled was intended to enter the rain field at 475 ft/sec and to exit at 200 ft/sec. The two runs were planned to overlap between 450 and 475 ft/sec.

Because of incorrect sled weight, the maximum velocity obtained during both tests was lower than planned. In the first test, the sled entered the rain field at 650 ft/sec (instead of 800 ft/sec) and exited at approximately 410 ft/sec. In the second test, the sled entered the rain field at 430 ft/sec (instead of 475 ft/sec) and exited at approximately 250 ft/sec. The test did furnish data in the rain field from 250 to 650 ft/sec for a total flight time of 10 sec in rain.

Calibration of the rain field showed that the rain rate for the test ranged from 20 to 24 in./hr. However, the wind during the post-run calibration was higher than the actual test conditions, so that the rain rate was probably somewhat higher than that for the calibration record.

After the rain test, each alternator was tested in the laboratory to provide a comparison with data taken before the test and to determine whether changes in device structure occurred from the rain.

4.4 Results

The functional characteristics of the generators in the rain field are summarized in figures 7 to 14. Figure 7 is a plot of telemetered voltage versus sled velocity and sled flight time for generator No. 6 during the high velocity run. The sled accelerates from rest and enters the rain field 2.1 sec later, at a velocity of 650 ft/sec. The figure shows that the generator output voltage from the telemetry system increases and reaches a maximum of 5.8 V before entering the rain field. The generator output is independent of sled velocity at the higher velocities, and no degradation of voltage appears during the 3.8 sec in the rain field. As the sled decelerates further after leaving the rain, the voltage decreases because the alternator rotational speed is decreasing.

The voltage output from the telemetry system at 600 ft/sec before entering the rain is 5.7 V and it is about 5.8 V in the rain field at the same velocity. This is a further indication that no degradation in output takes place as a result of the rain. The voltage at 300 ft/sec on the acceleration portion of the run is about 3.7 V, whereas the voltage at 300 ft/sec on the decelerating portion of the run is about 5.2 V. This variation is due to the inertia of the rotor which causes a delay in the rotational speed change as the air velocity changes.

Figure 8 is a plot of voltage versus sled velocity and time of travel for alternator No. 6 in the low-speed run. The sled enters the rain field at a

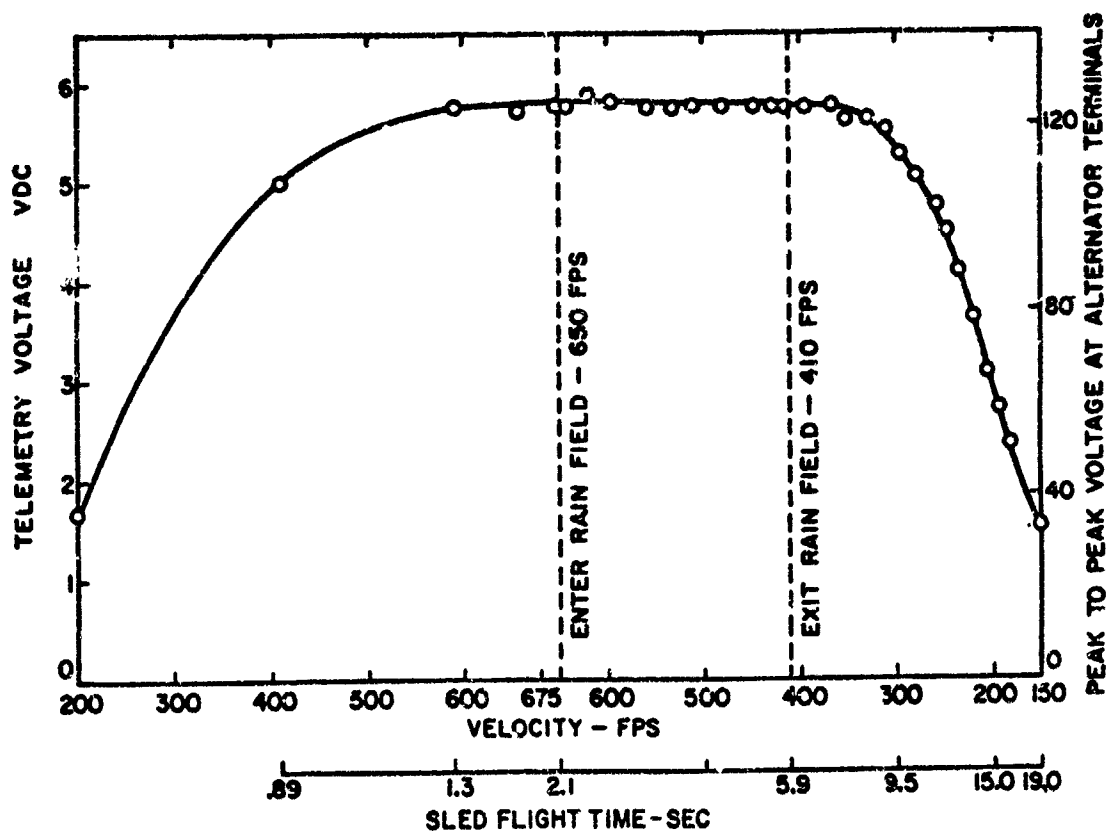


Figure 7. High-velocity run in rain field for alternator No. 6.

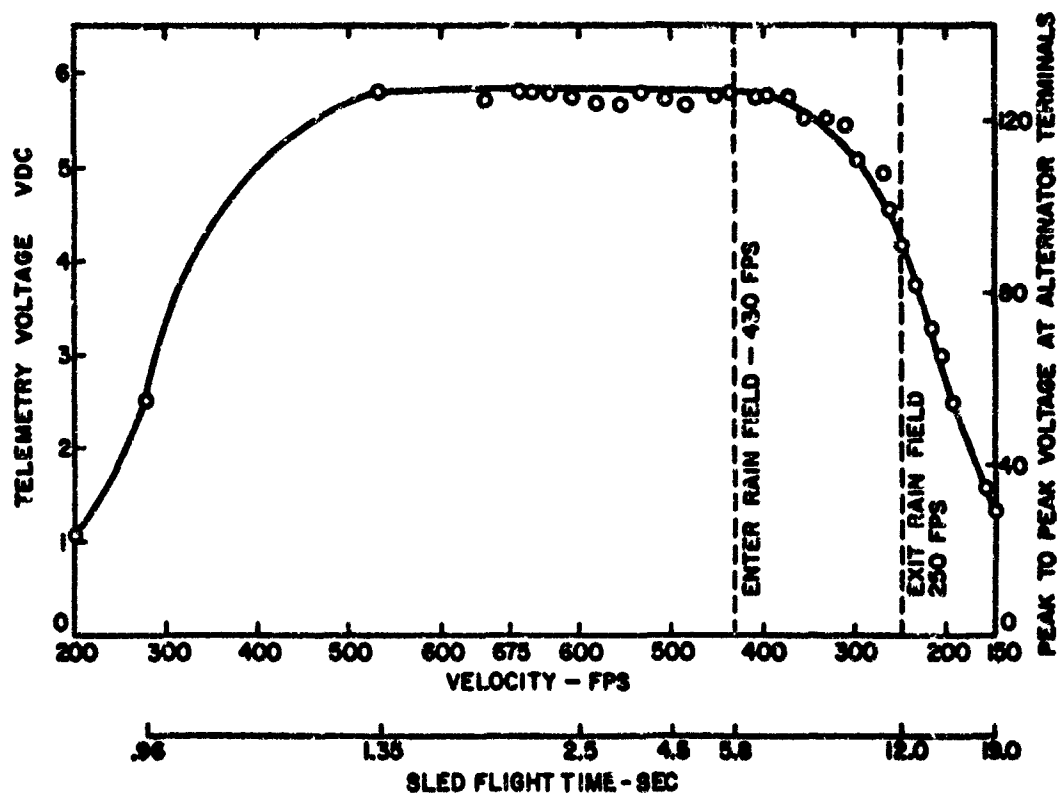


Figure 8. Low-velocity run in rain field for alternator No. 6.

velocity of 430 ft/sec at 5.8 sec after launch on the decelerating portion of the run, and leaves the rain field 6.18 sec later at a velocity of 250 ft/sec. There is no sharp drop in the output as the alternator enters or leaves the rain field, thus showing that the alternator is unaffected by the rain.

Hence, figures 7 and 8 show that the alternator functioned in the rain field for a duration of 10 sec over a velocity range of 250 to 650 ft/sec and suffered no degradation of output. Similar results hold for the other alternators tested, as shown in figures 9 to 14.

All alternators were tested in the laboratory before and after the rain test to ascertain whether any permanent damage had been caused by the rain. The results are presented in Table I. The outputs of the alternators were the same after the test as before, indicating that no permanent damage occurred as a result of the test.

5. TEMPERATURE TESTS OF 60-MM ROTARY POWER SUPPLY FROM -60° TO +160°F

5.1 Purpose

Laboratory tests were conducted to determine the effect of temperatures between -60° to +160°F on the alternator performance. The effect of the working gas temperature on power was studied.

5.2 Experimental Apparatus and Procedure

The alternator was mounted in a test chamber as shown in figure 15, with instrumentation in figure 16. The chamber temperature was controlled from -60° to +160° F, and the working fluid for the test was compressed nitrogen, which has physical properties similar to air. The nitrogen gas was passed through two copper coils in the oven, so that the nitrogen temperature was nearly identical to the oven temperature before entering the generator.

The instrumentation diagram for the test is shown in figure 17. The temperature of the working gas was monitored in the settling chamber by a chromel-alumel thermocouple and the pressure in the settling chamber was monitored by a pressure transducer.

For each run, the settling chamber was heated to the required temperature and kept at that temperature for 30 min to equalize temperature of the oven and that of the gas in settling chamber. The pressure of the supply gas was increased from zero up to six lb/in.² above atmospheric pressure.

For each pressure setting, the frequency and power output of the alternator were monitored with an x-y recorder. The settling tank and chamber temperatures were recorded before and after each test to ensure that the temperature did not change significantly during the run and that the settling-tank temperature was equal to that of the oven.

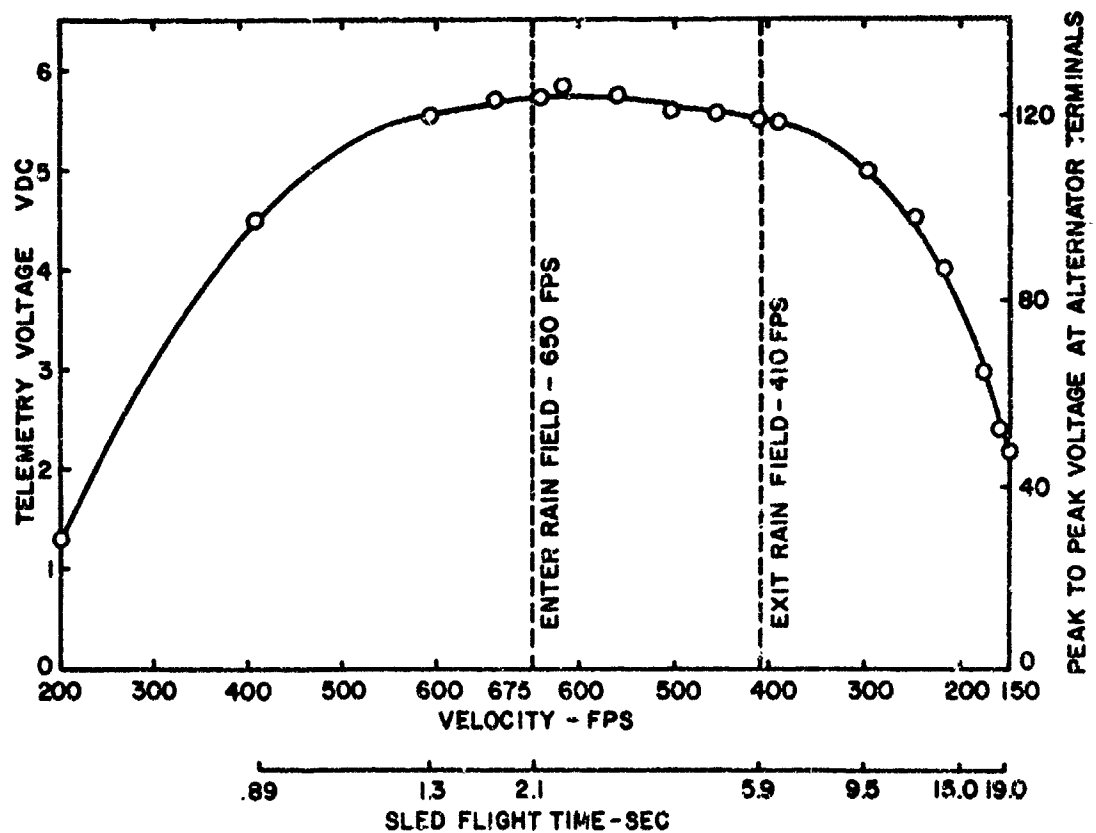


Figure 9. High-velocity run in rain field for alternator No. 7.

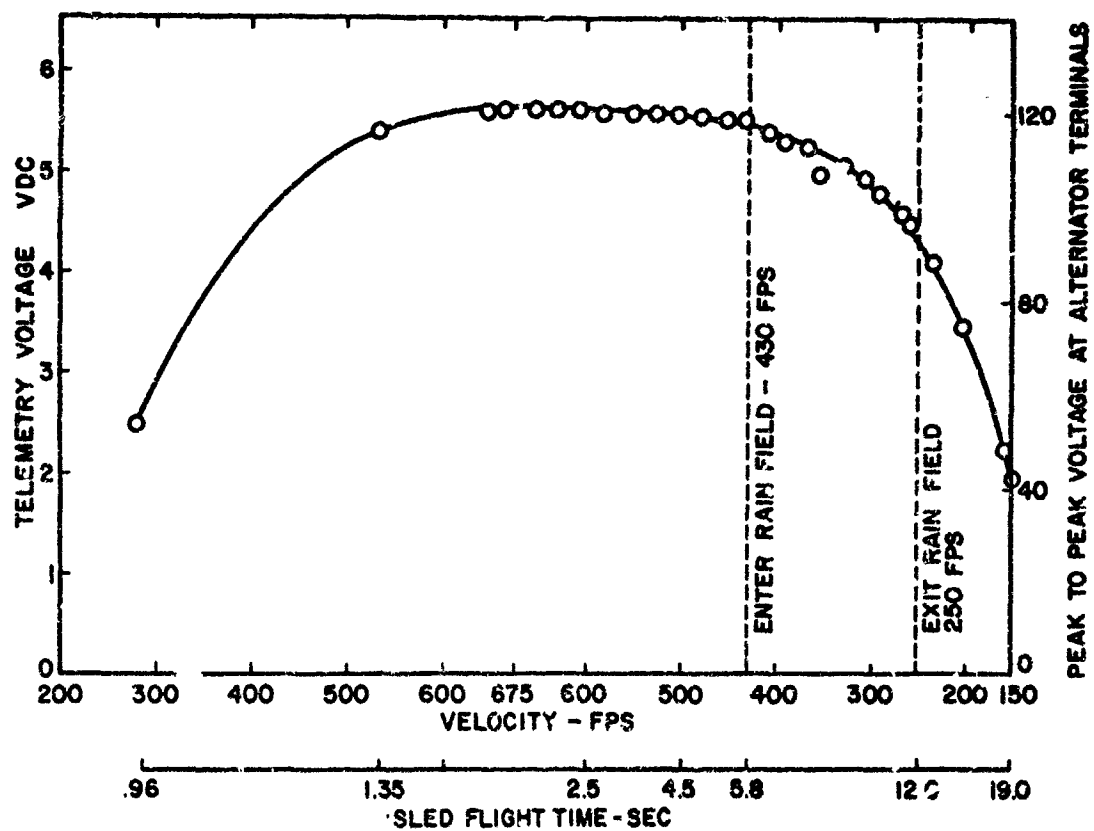


Figure 10. Low-velocity run in rain field alternator No. 7.

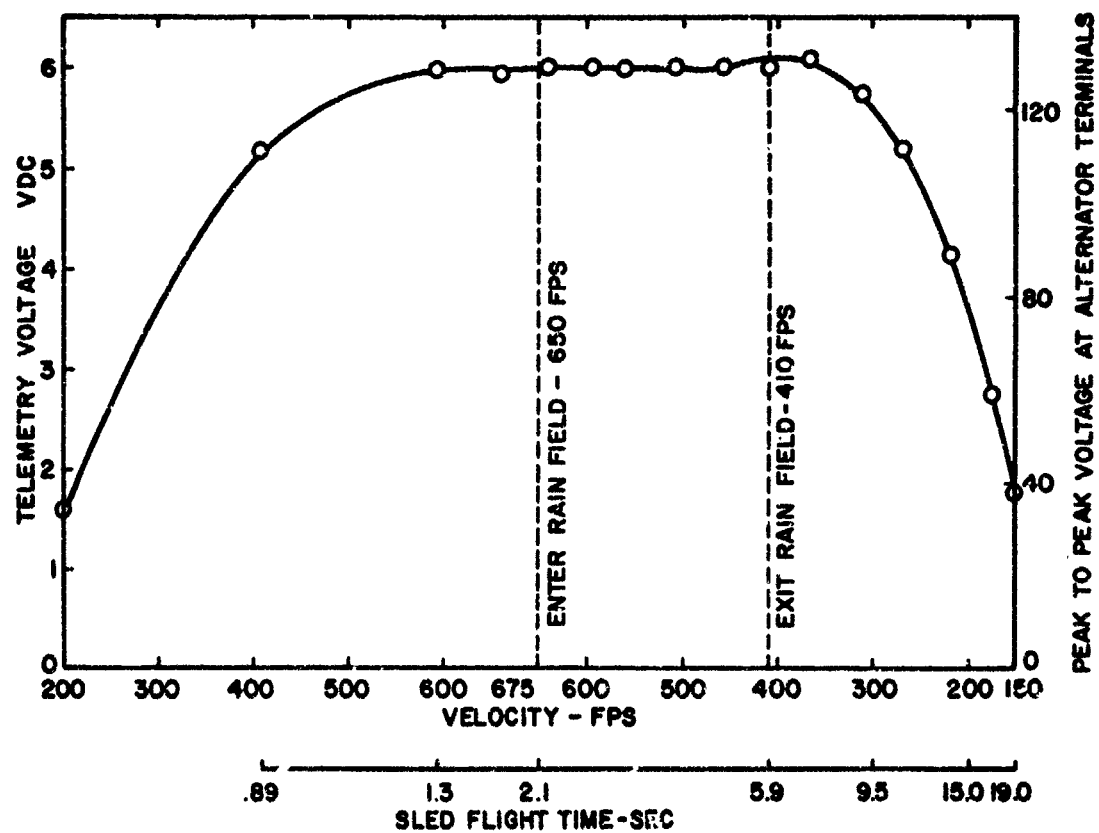


Figure 11. High-velocity run in rain field alternator No. 8.

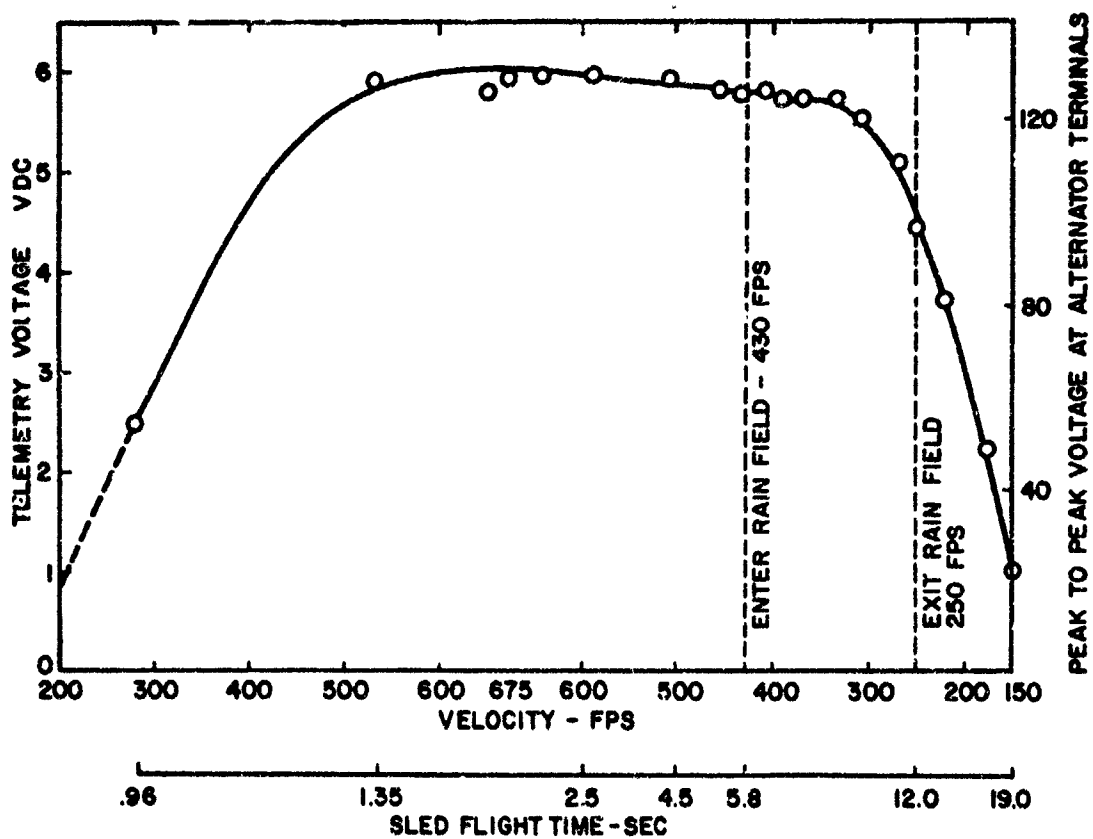


Figure 12. Low-velocity run in rain field for alternator No. 8.

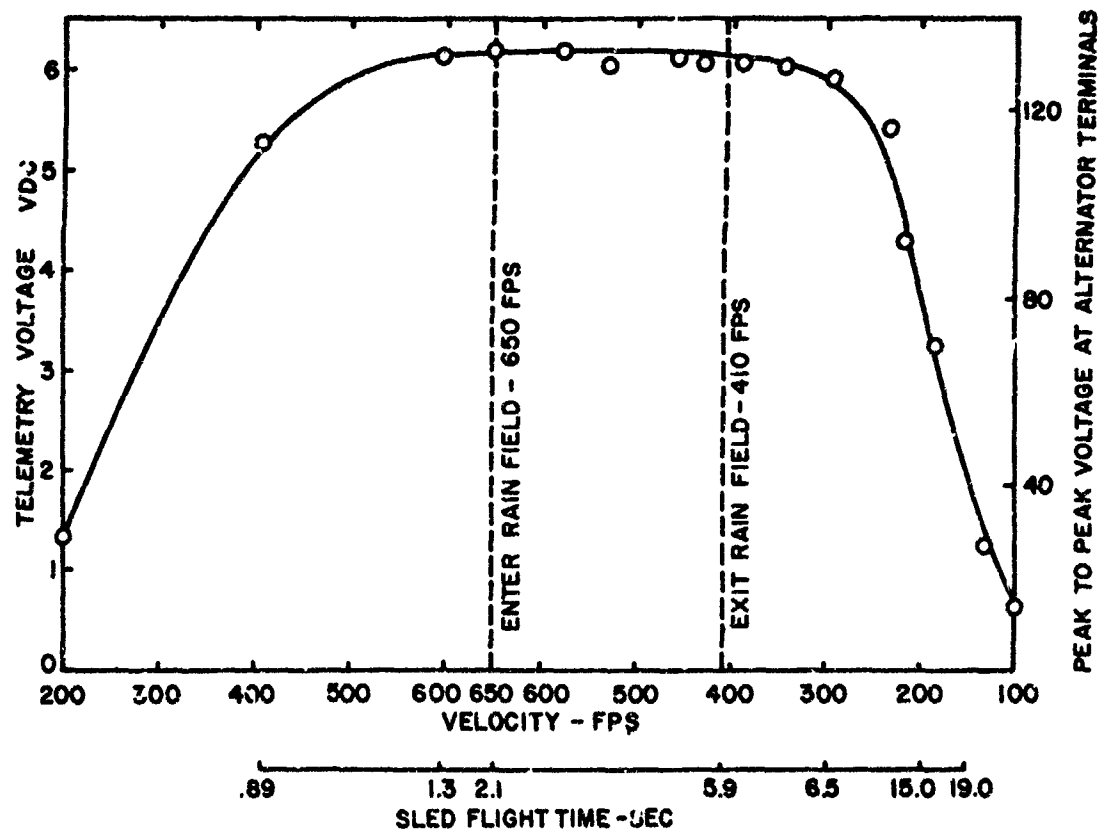


Figure 13. High-velocity run in rain field alternator No. 9.

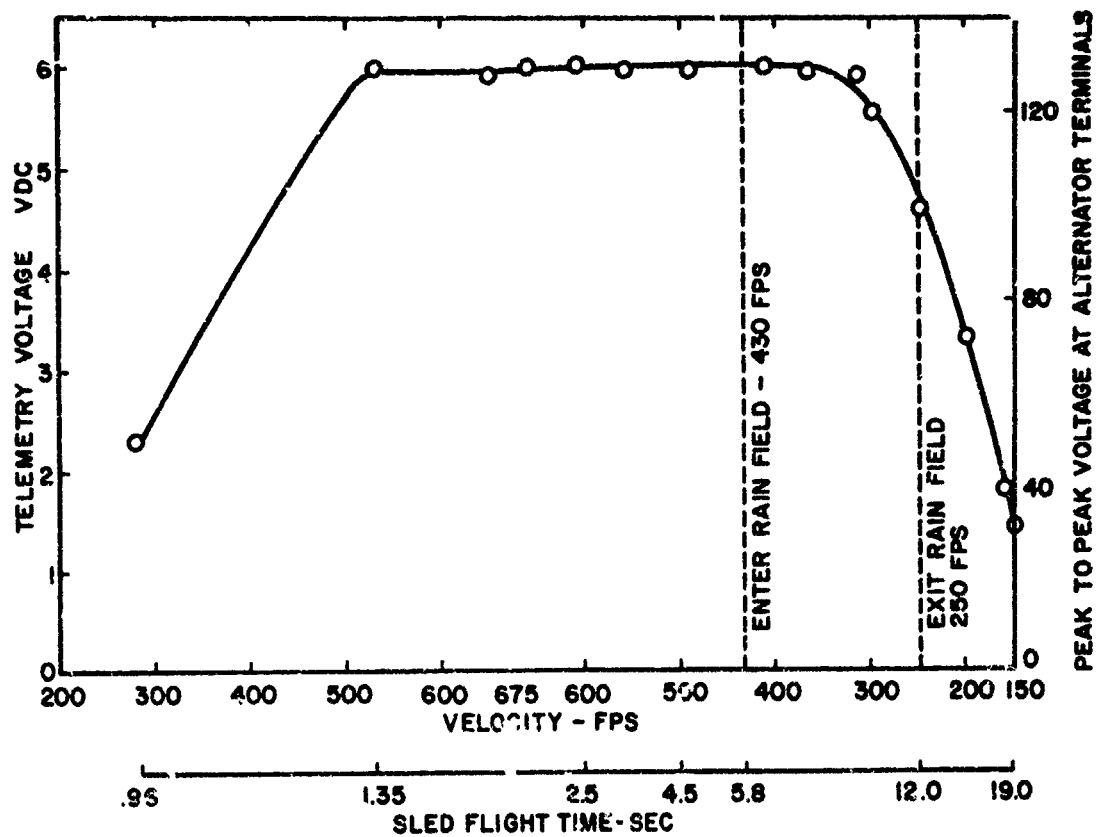


Figure 14. Low-velocity run in rain field for alternator No. 9.

**TABLE I. LABORATORY COMPARISON OF ALTERNATOR OUTPUT
BEFORE AND AFTER RAIN TEST**

Alternator	Velocity (FPS)	Output Of Reducing Circuit (Volts, dc)	
		Before Rain Test	After Rain Test
6	110	1.2	1.2
6	156	2.4	2.7
6	191	3.8	4.0
6	270	5.4	5.4
6	311	5.8	5.7
6	348	6.0	5.9
7	110	1.5	1.6
7	156	2.9	3.1
7	191	3.8	4.0
7	270	4.6	4.9
7	311	4.8	5.1
7	348	5.0	5.2
8	110	1.2	1.4
8	156	3.0	3.0
8	191	4.1	4.2
8	270	5.4	5.5
8	311	5.7	5.8
8	348	5.9	5.9
9	110	1.2	1.4
9	156	2.9	2.9
9	191	4.1	4.2
9	270	5.6	5.6
9	311	5.9	6.0
9	348	6.0	6.1
9	478	6.5	6.5
9	575	6.6	6.6
9	652	6.7	6.7
9	716	6.8	6.7

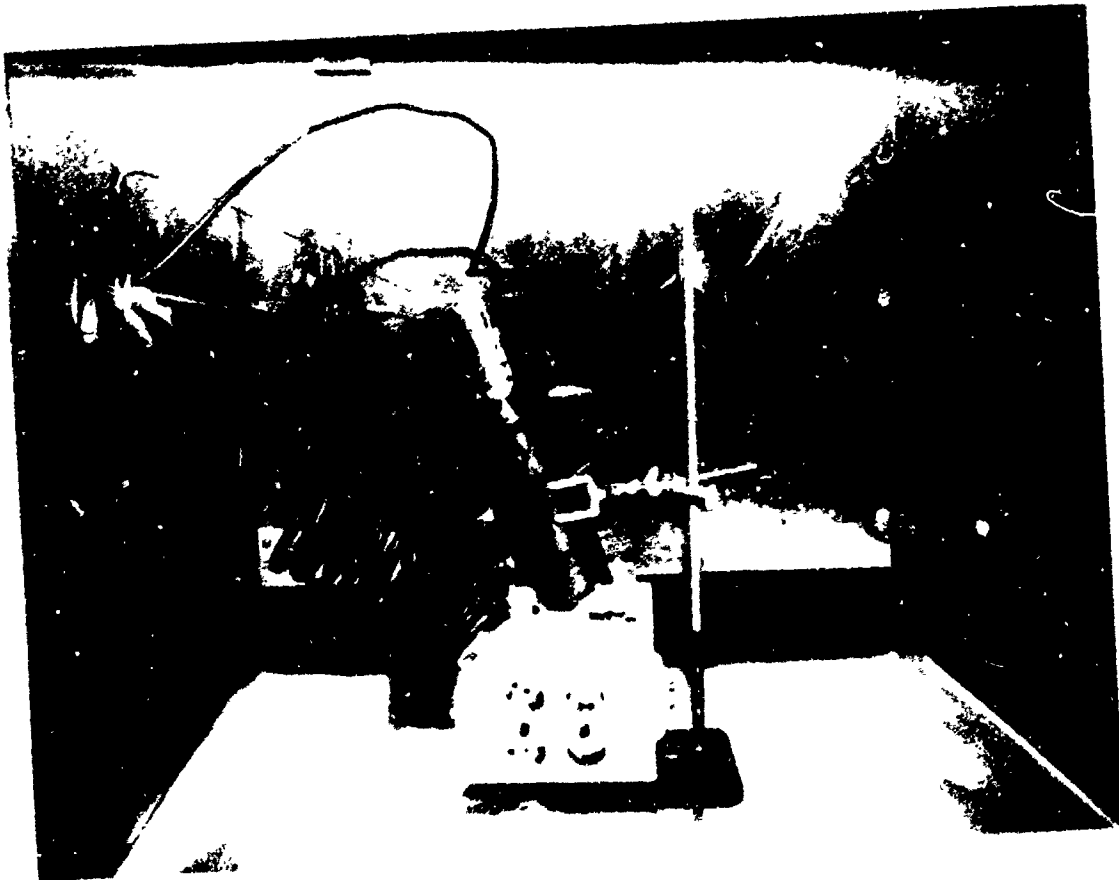


Figure 15. Alternator mounted in temperature test chamber.

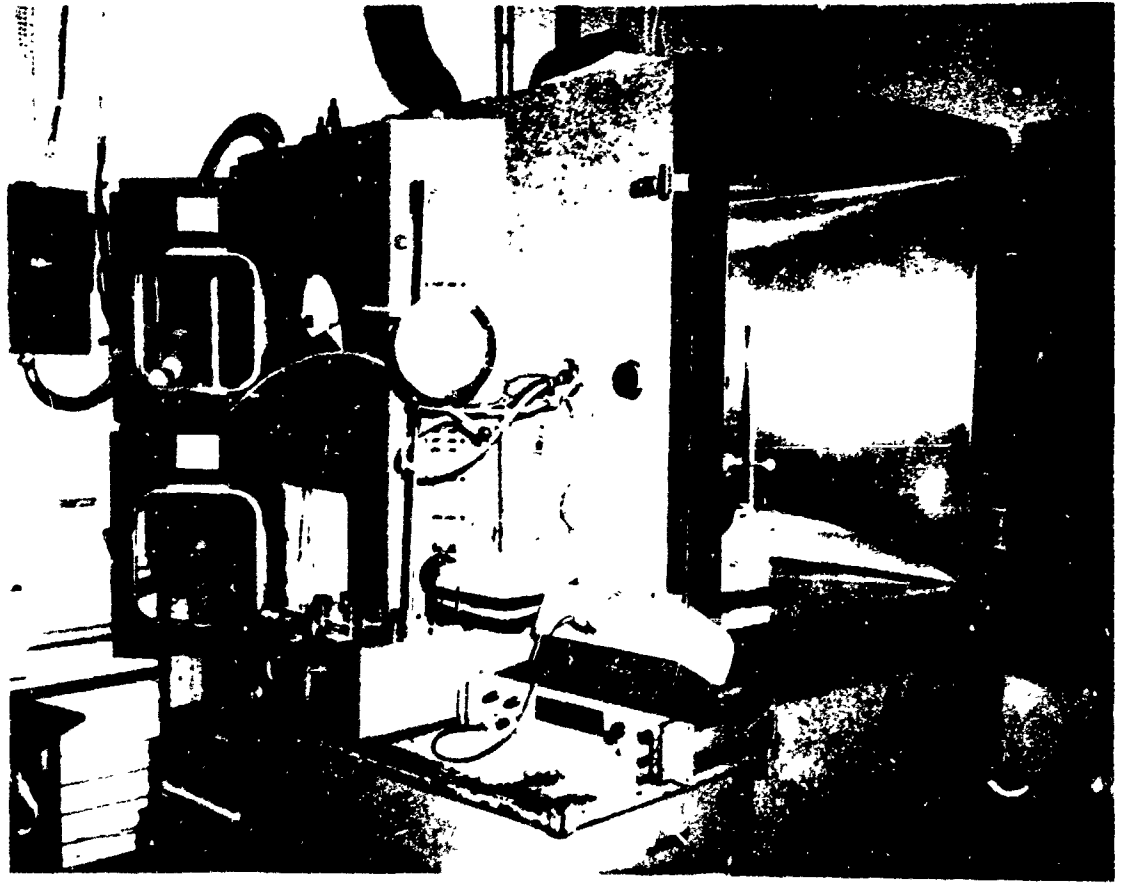


Figure 16. Instrumentation for temperature test of alternator.

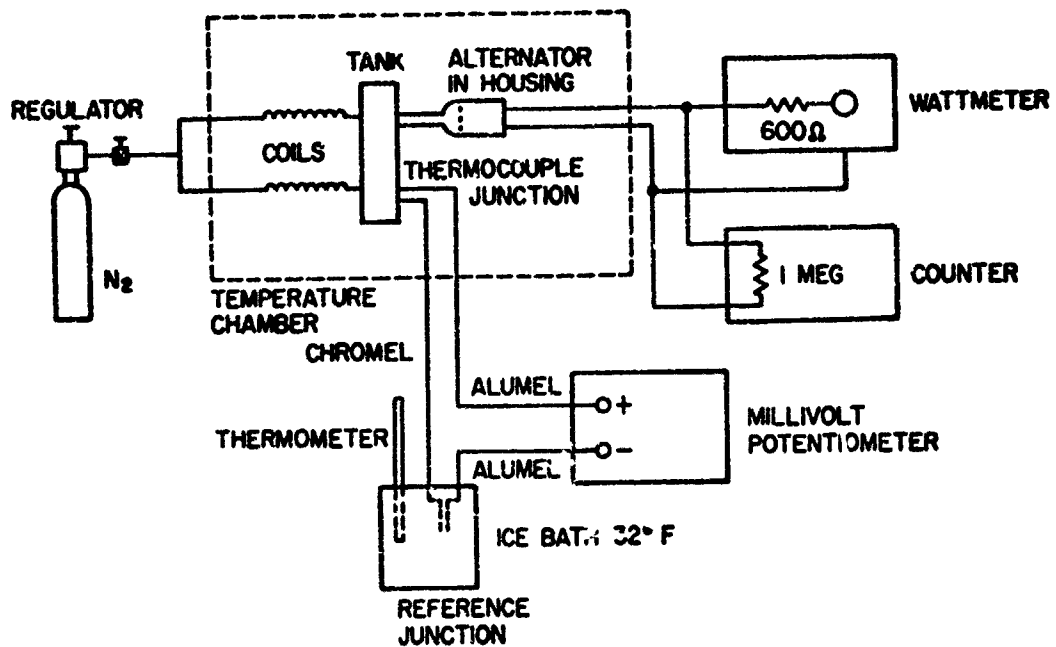


Figure 17. Experimental arrangement for studying effect of temperature on alternator output.

This procedure was repeated for temperatures of -60° , -40° , -20° , 0° , 32°F , room temperature, 100° , 125° , and 160°F . For the tests, four alternators were chosen at random from a total of 20.

Because the gas density is a function of temperature, the measured supply gas velocity had to be compensated for temperature to compare it with the laboratory data at ambient conditions. The inlet gas velocity is calculated in terms of the laboratory pressure by

$$V = \sqrt{\frac{2\Delta P}{\rho}} \quad (1)$$

where

V = velocity at temperature T

ΔP = dynamic pressure being supplied to alternator

ρ = air density at temperature T

At constant pressure, the absolute temperature and density are related to the reference values P_r and T_r by the ideal gas law

$$\rho T = \rho_r T_r$$

or

$$\rho = \frac{T_r}{T} \rho_r$$

Where ρ_r is the density at room temperature, and T_r is room temperature. Substituting this expression in (1) gives

$$V = \sqrt{\frac{2\Delta P}{\rho}} = \sqrt{\frac{2\Delta P}{\rho_r}} \left(\frac{T}{T_r}\right) = \left(\frac{T}{T_r}\right)^{1/2} V_r \quad (2)$$

This formula relates the velocity at supply gas temperature different from room temperature to the dynamic pressure ΔP measured in the laboratory.

Several alternators were tested. Typical results of output power as a function of inlet air velocity for the extreme temperatures -60° to $+160^{\circ}\text{F}$ are shown in figure 18 for alternator No. 32. From the figure it is seen that the generator produced 0.5 W of power into a 600- Ω load at a velocity of 156 ft/sec at room temperature. By increasing the temperature of the working gas to 160°F , the output power at 156 ft/sec drops to 0.425 W, a reduction of 15 percent. At the velocity of 200 ft/sec, there appears to be no change in output power between room temperature (90°F) and 160°F . At the lower temperatures (-60°F), the generator produces 0.645 W (fig. 18), an increase of about 20 percent above the power measured at 156 ft/sec at room temperature. The increase in output power at the low temperature is attributed to a density increase, that augments the mass flow entering the generator.

The other alternators tested showed the same trends under the influence of temperature changes as that shown in figure 18.

6. WIND TUNNEL TEST OF ALTERNATOR PERFORMANCE

6.1 Introduction

To check alternator performance under simulated flight conditions, wind-tunnel tests were conducted at the Picatinny Arsenal wind tunnel facility. These tests provide information on the effect of projectile angle of attack and Mach number on the alternator performance. The alternator performance in the wind tunnel at zero angle of attack was then compared with that obtained with a laboratory test rig.

6.2 Description of Test

The Picatinny Arsenal subsonic wind tunnel facility used for the test has a 24-in. test section which can accommodate a 60-mm M49A4E1 mortar projectile with a 4.82-in. tail section. The projectile was mounted on a strut with variable angle of attack. Electrical leads from the alternator, mounted in the projectile nose section, were connected to a frequency meter that produced a d-c voltage output proportional to frequency that was recorded on an x-y plotter. The experimental arrangement is shown in figure 19. Test runs were conducted at Mach numbers of 0.2, 0.3, 0.39, and 0.63, and at angles of attack of 0, 4, 10, and 15 deg. Alternators were installed in two fuze configurations (fig. 20, and 21) designated as HDLD and ABCA. The two configurations differ in aerodynamic shape in that the exhaust holes in the HDLD design are located on the spherical nose behind a flange, whereas the holes on the ABCA are positioned on a conical surface without a flange.

Prior to the tunnel tests, the alternators were positioned in the two fuze ogives and calibrated in a laboratory test arrangement (fig. 22) that measured power output and rotational speed of the alternators as a function of inlet-air velocity. The laboratory results were then compared with those obtained in the wind tunnel.

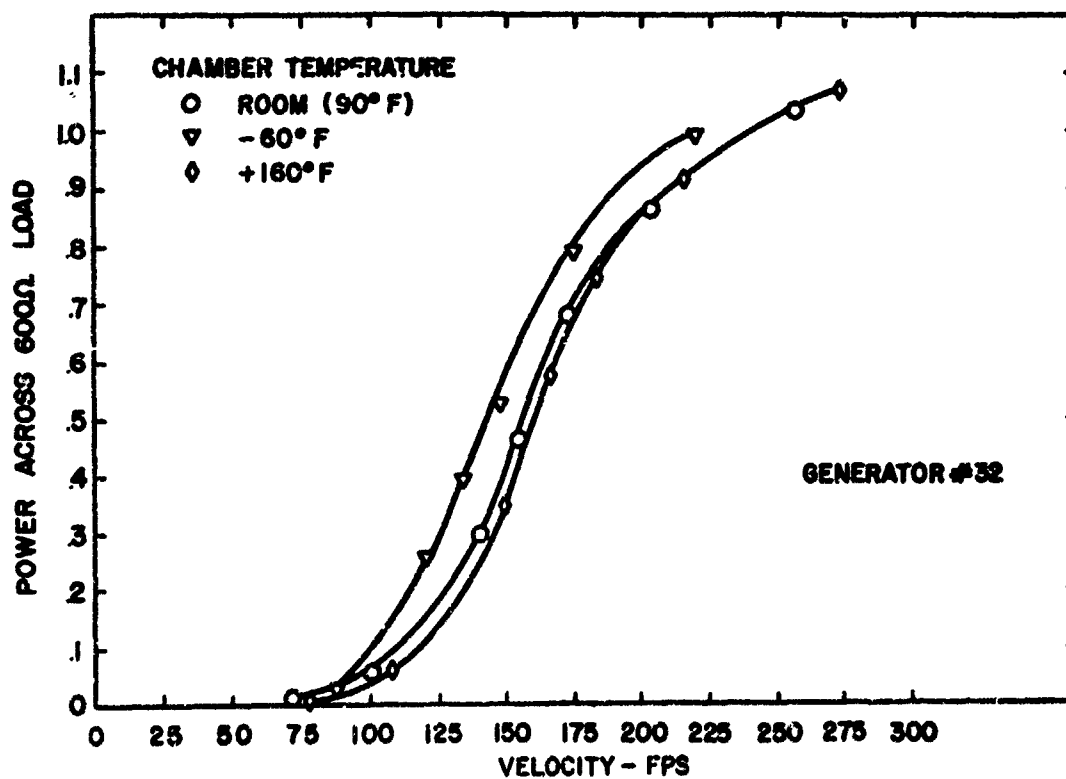


Figure 18. Power output versus velocity for three values of inlet gas temperature.

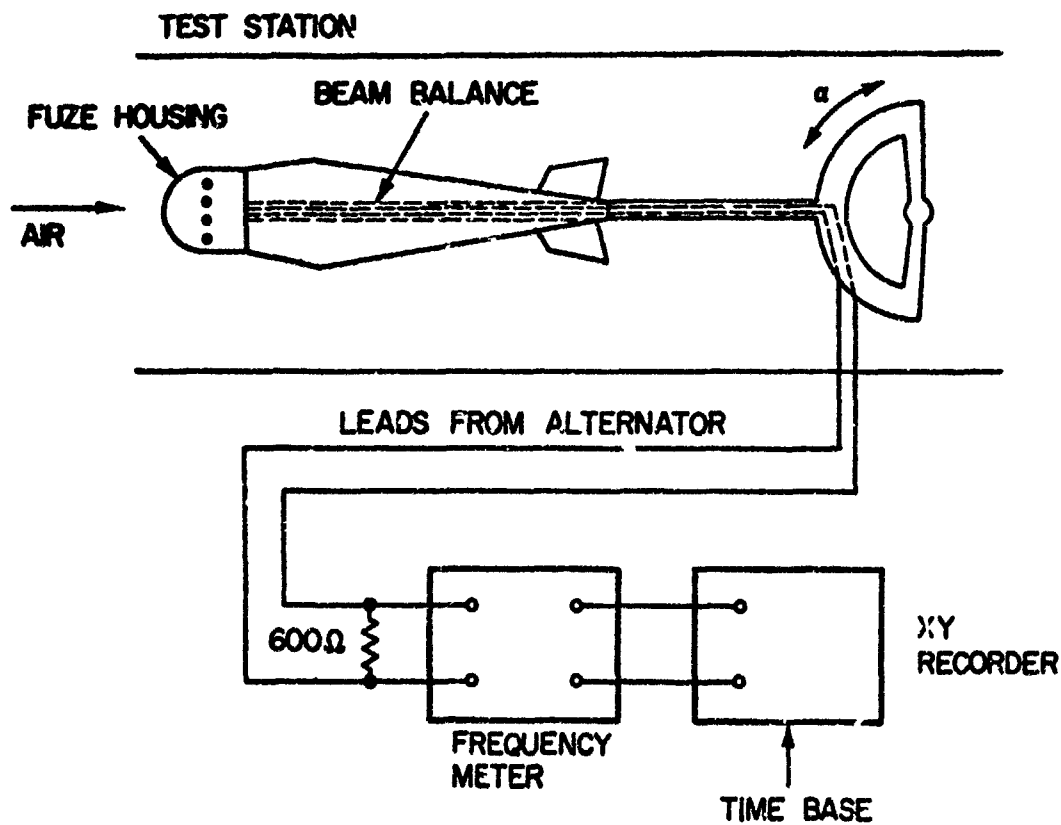


Figure 19. Apparatus for measuring alternator rotational speed versus velocity in wind tunnel.



Figure 20. HDLD fuze ogive.



Figure 21. ABCA fuze ogive.

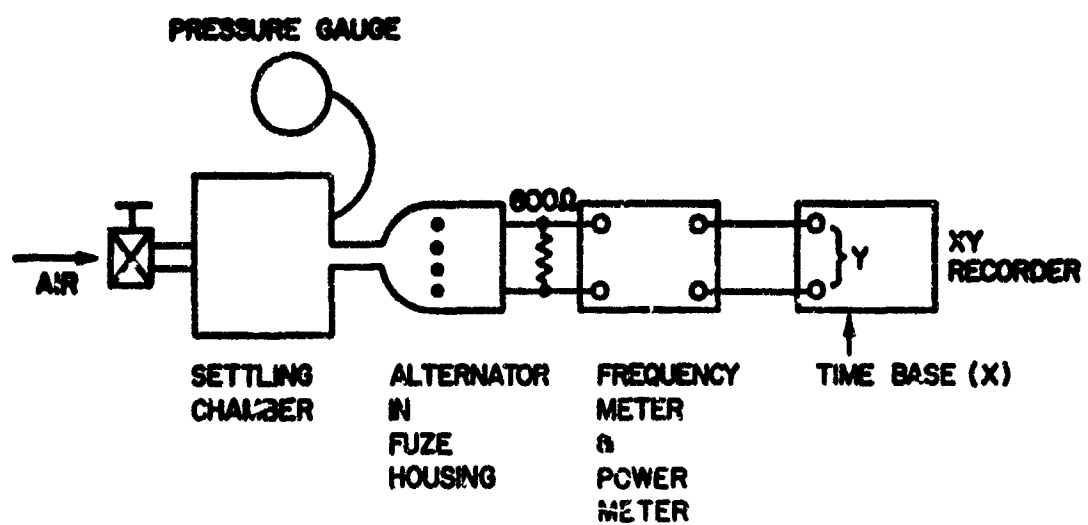


Figure 22. Laboratory test arrangement.

6.3 Wind Tunnel Test Results

The rotational speed of the alternator in the HDLD fuze ogive was measured in the laboratory and in the wind tunnel at 0-deg angle of attack. The results are shown in figures 23 and 24, in which rotational speed is plotted versus velocity. The data points from the laboratory and the wind tunnel can be connected by straight lines having the same slope; these lines are identical over the velocity range tested, and the maximum variation is no greater than five percent. The discrepancy between the laboratory data and that from the tunnel is caused by a variation of the static pressure at the ogive exhaust ports. The pressure at the exhaust ports is atmospheric while in the laboratory test fixture. In the wind tunnel it is different from atmospheric and is determined by the fluid boundary layer pressure, which depends on the fuze ogive geometry. The result is that the rotational speed at a given inlet velocity is higher in the laboratory than in the wind tunnel. The two graphs for the ABCA ogive are straight lines as in the previous case. The difference between the tunnel and test arrangement, however, is a maximum of ten percent. This difference arises from an increase in static pressure at the ogive exit port. The increase in static pressure at the exhaust ports in the wind tunnel arises from the cone-surface pressures of the ABCA fuze ogive. In general, the laboratory and tunnel measurements show that the laboratory test apparatus provides a good indication of the alternator's performance at 0-deg angle of attack.

Figure 25 is a curve of rotational speed of the alternator in the HDLD fuze ogive versus angle of attack for variations in the wind-tunnel velocities. The graphs are straight lines with negative slopes. The rotational speed at a velocity of 223 ft/sec ($M = 0.2$) decreases from 367 rps at 0-deg angle of attack to 250 rps at 15-deg angle of attack, a reduction of 32 percent. The rotational speed at an inlet velocity of 678 ft/sec varies from 1850 rps to 1633 rps, a change of 12 percent. These data indicate that the rotational speed during flight will be reduced up to 32 percent for variations in flight attitude between 0° and 15° , using the HDLD fuze ogive.

Measurements of alternator rotational speed were also conducted in the wind tunnel using the ABCA fuze ogive. Figure 26 summarizes the measured rotational speeds versus angle of attack at various inlet velocities. Note that the slope of the lines for the ABCA ogive remains nearly constant over the velocity range, whereas these slopes decreased with increasing velocity with the HDLD fuze ogive. The rotational speed change at 223 ft/sec ($M = 0.3$) is from 333 rps at $\alpha = 0$ deg to 262 rps at $\alpha = 15$ deg, a decrease in rotational speed of 21 percent as compared with 32 percent for the HDLD. At a tunnel velocity 678 ft/sec, the rotational speed increases from 1806 rps at $\alpha = 0$ deg to 1833 rps at $\alpha = 15$ deg, an increase of 1.5 percent as compared with a 12-percent reduction for the HDLD. The ABCA cone configuration causes up to 21-percent reduction in rotational speed at the low velocities for variation in flight attitude of 0 to 15 deg, but the rotational speed is independent of attitude at the higher velocities.

The tunnel tests show that the final configuration for the MOFM fuze should be designed with some of the characteristics of the ABCA fuze ogive, so that the losses of alternator rotational speed at various angle of attack will be minimized.

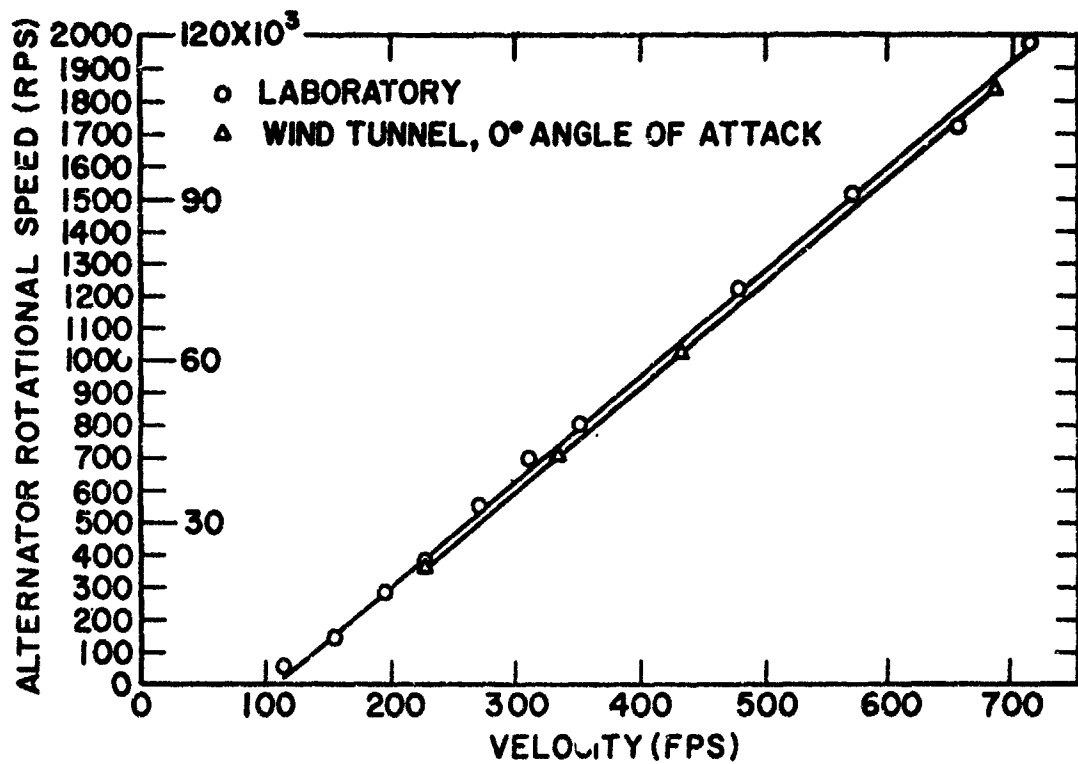


Figure 23. Alternator rotational speed in laboratory and in wind tunnel—HDLD ogive.

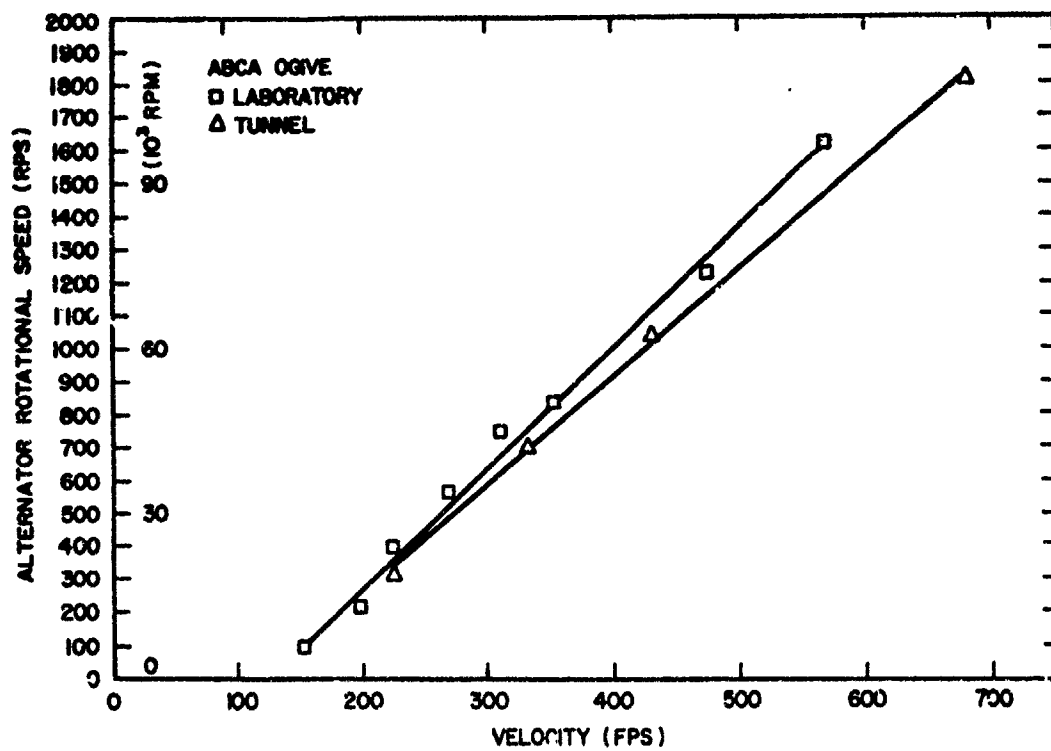


Figure 24. Alternator rotational speed in laboratory and in wind tunnel—ABCA ogive.

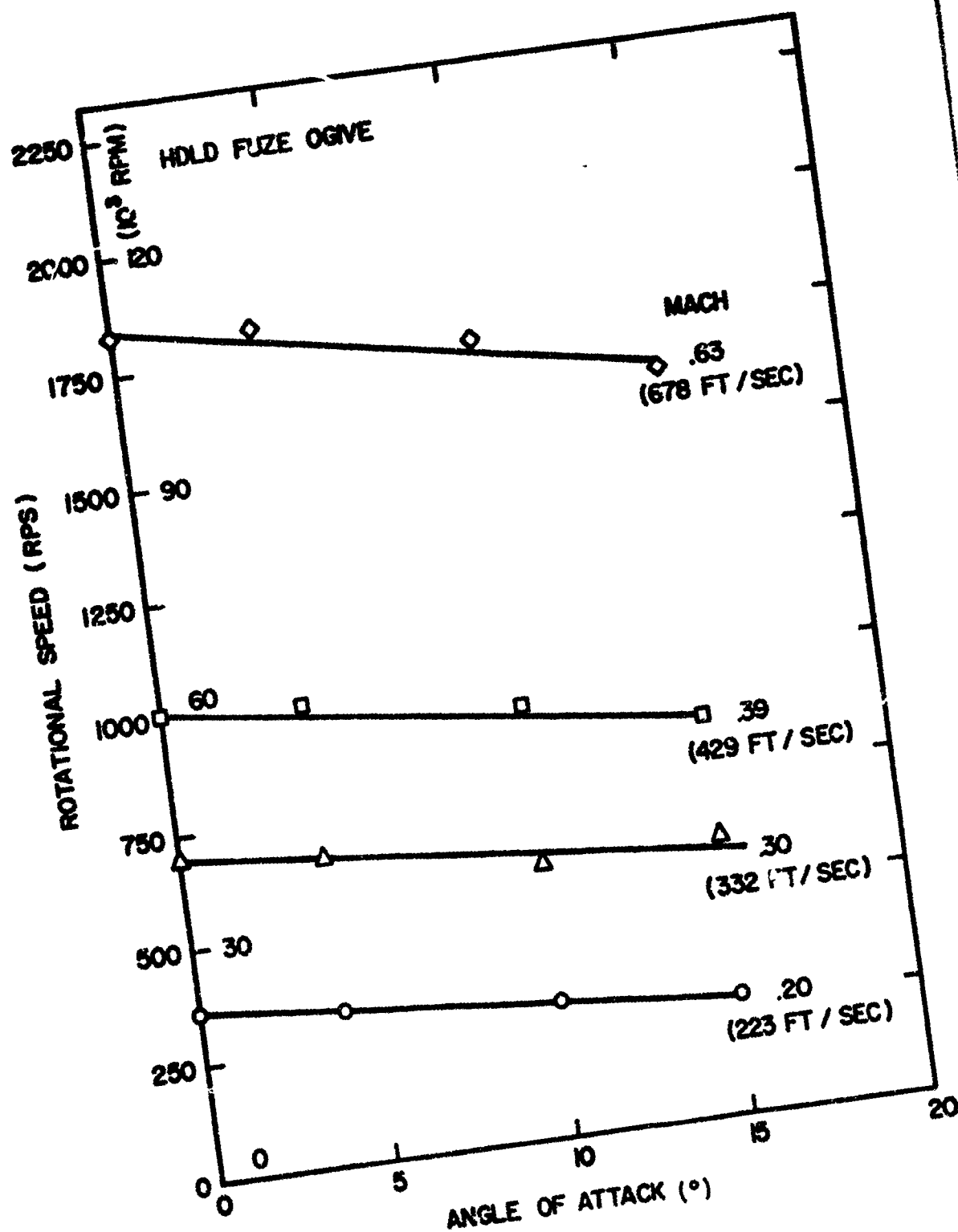


Figure 25. Rotational speed versus angle of attack at mach numbers of 0.20, 0.30, 0.39, and 0.63 for HDLD fuze ogive.

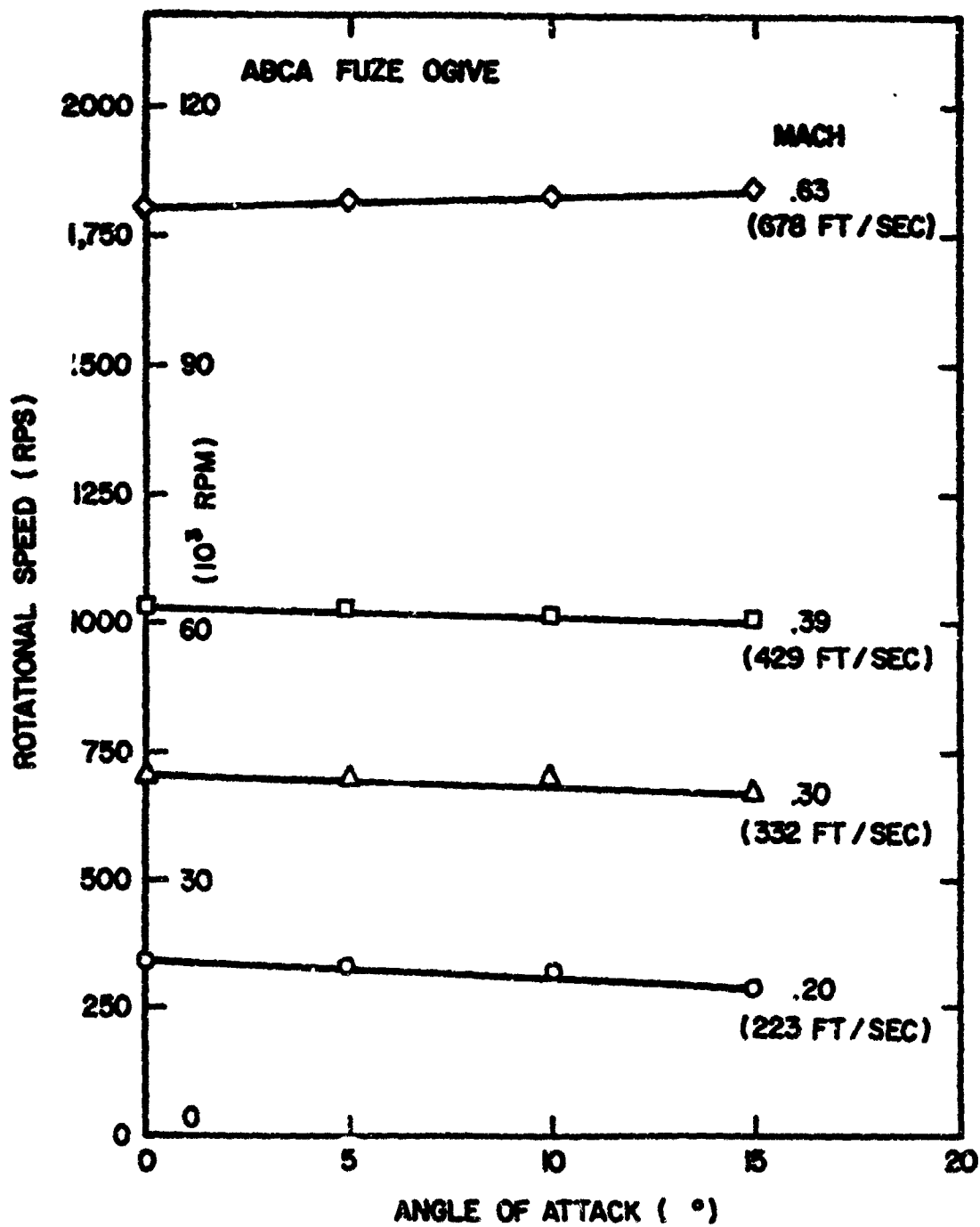


Figure 26. Rotational speed versus angle of attack at mach numbers of 0.20, 0.30, 0.39, and 0.63 for ABCA fuze ogive.

7. DEVELOPMENT OF 600 SERIES ALTERNATOR

7.1 Stator Design

The tests previously described were conducted with 500 series alternators, which contained a rotor 0.560 in. in diameter by 0.250 in. length. To achieve a design amenable to high-production stamping techniques, a second type of alternator, the 600 series, was developed (fig. 27). This device has a rotor 0.600 in. in diameter and 0.200 in. in length. The stator pole pieces are shorter than the pole pieces of the 500 series design and, hence, can be drawn in a stamping process from the stator base.

Three sets of stator casings were made having pole widths of 0.250 in., 0.275 in., and 0.292 in. The respective alternator starting velocities were 100, 85, and 49 ft/sec. The 0.292-in.-wide stator was most desirable because it had the lowest starting velocity required to drive the safing-armling system.

The power output at the lower velocities was about the same for all stator pole widths as shown in the power-versus-velocity plot in figure 28. All alternators produce about 0.550 to 0.600W at 150 ft/sec, and there is no noticeable difference in output power at velocities up to 190 ft/sec. At the higher velocities, the power is less with the wider poles. The alternator with 0.250-in.-width pole pieces produces about 12 percent more output than the one with the 0.292-in. poles. For the 60-mm mortar application, it is desirable that the alternator not produce excessive power at the higher velocities. Therefore, the stator configuration with the pole width of 0.292 in. was chosen.

7.2 Magnet Rotor Design

The effect of magnet-rotor length on output power is shown in figure 29, a plot of electrical power output versus velocity. For this test, the stator-pole width of the alternator was 0.250 in. Rotors made from sintered Alnico 2 having lengths of 0.200 and 0.280 in. were tested. The 0.200 in. height rotor produces 0.550W at 150 ft/sec. The generated power is 0.400W with the 0.280 in. height rotor; this power is below the fuze requirement. Hence, the 0.200 in. length rotor was selected for use on the 600 series alternator design.

Figure 30 shows the output power and rotational speed of the selected design (pole width is 0.292 in. and rotor length is 0.200 in.) over the operating range of the 60-mm mortar. The generator produces 0.800W at 150 ft/sec and 2.2W at 575 ft/sec. The steady-state rotational speed increases linearly with velocity and reaches a maximum of 152,000 rpm at 772 ft/sec.

7.3 Tests With Alnico 6

To examine the effect of magnetic materials, several rotors made from Alnico 6 were tested. Figure 31 shows the output power into a 600- Ω load using an Alnico 6 magnet rotor having a 0.247-in. magnet length. The power

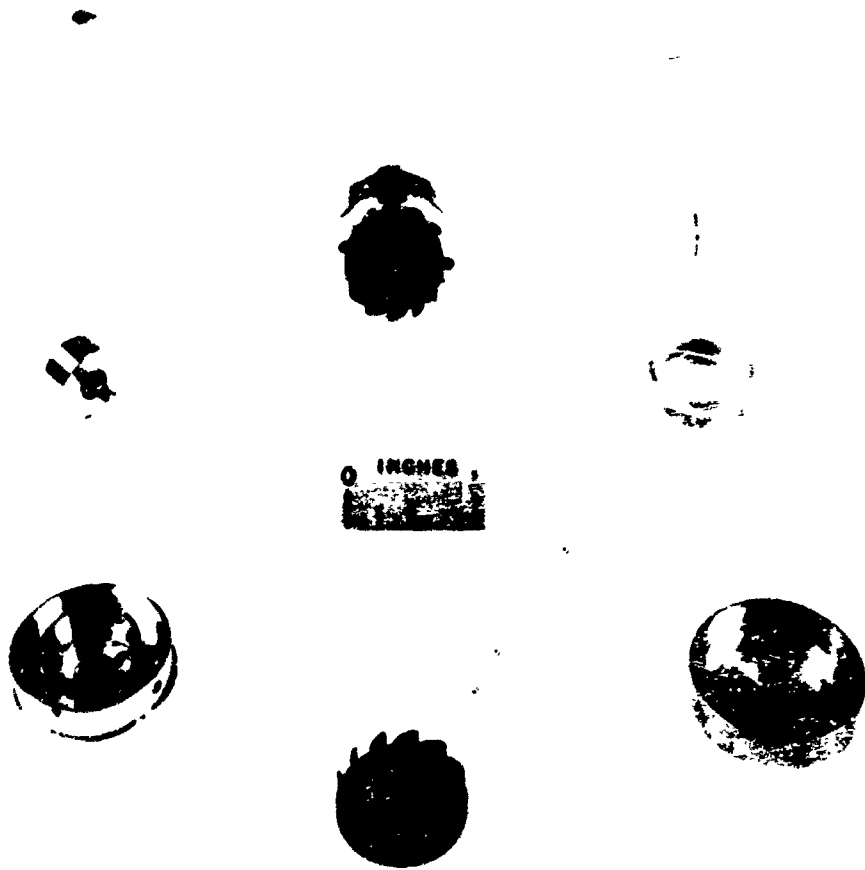


Figure 27. 600 series alternator components and assembly.

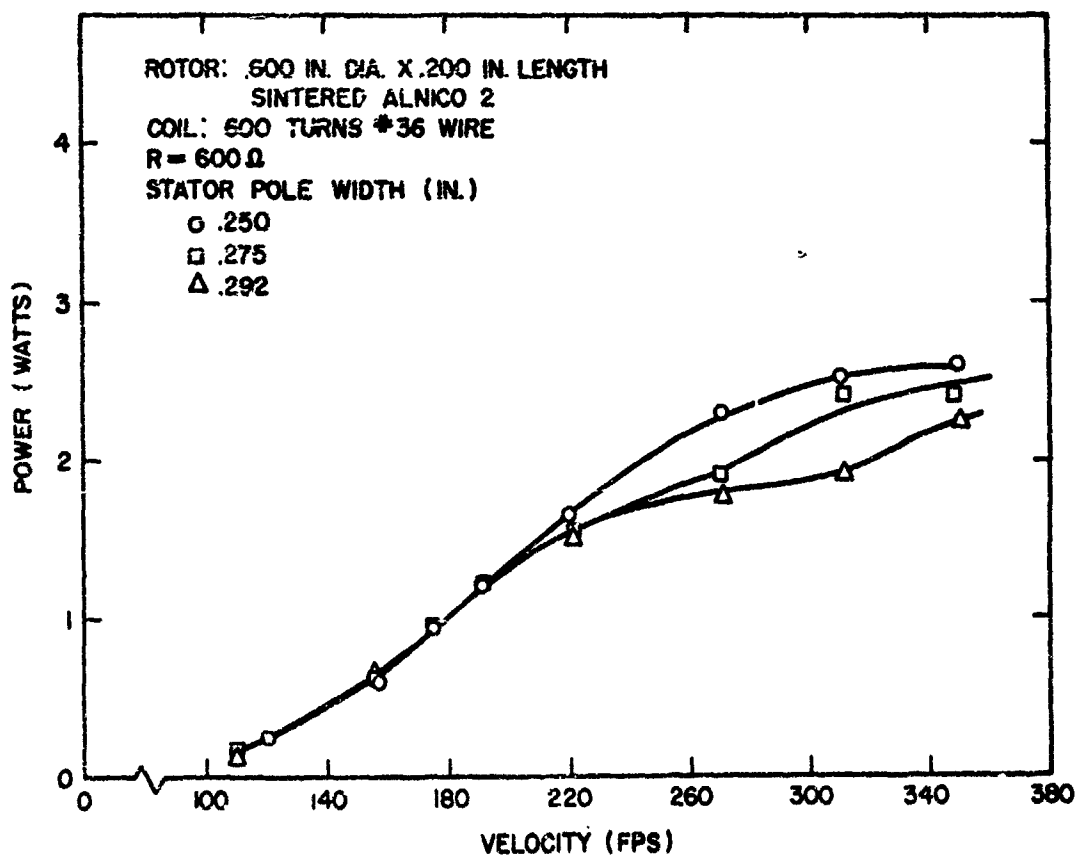


Figure 28. Electrical power versus velocity for various stator pole widths.

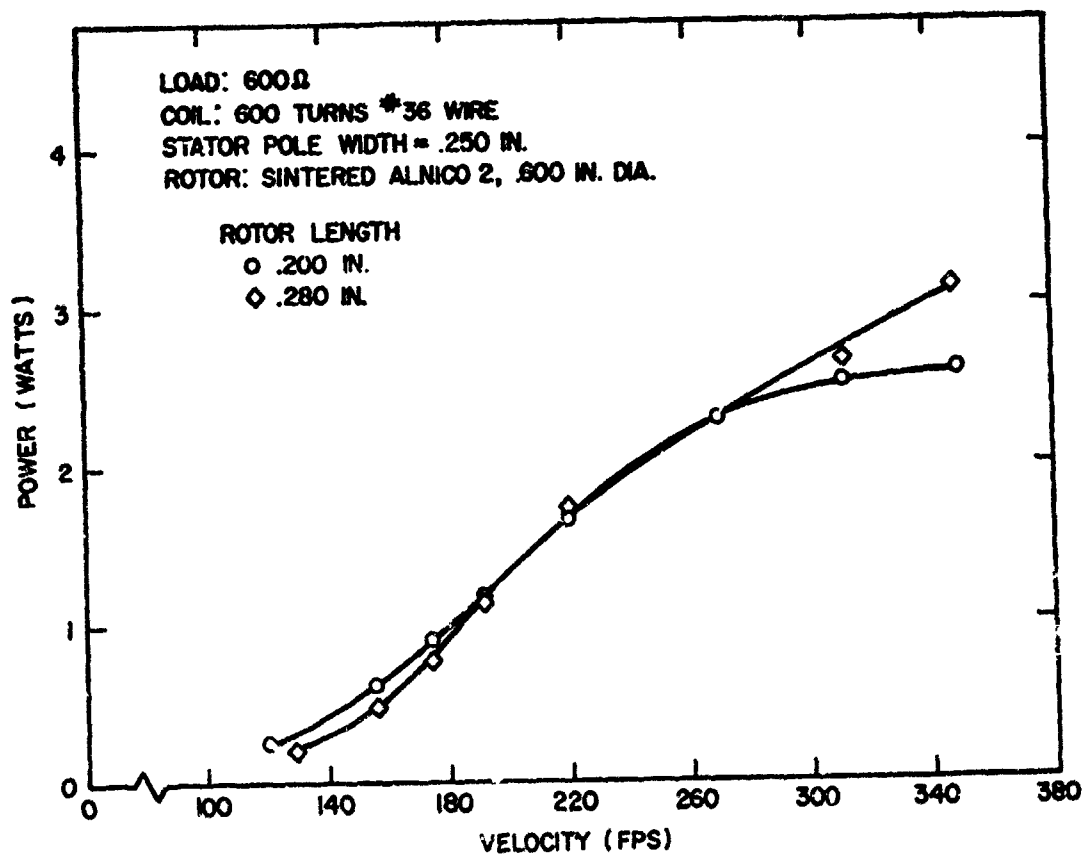


Figure 29. Electrical power versus velocity for rotors with different lengths.

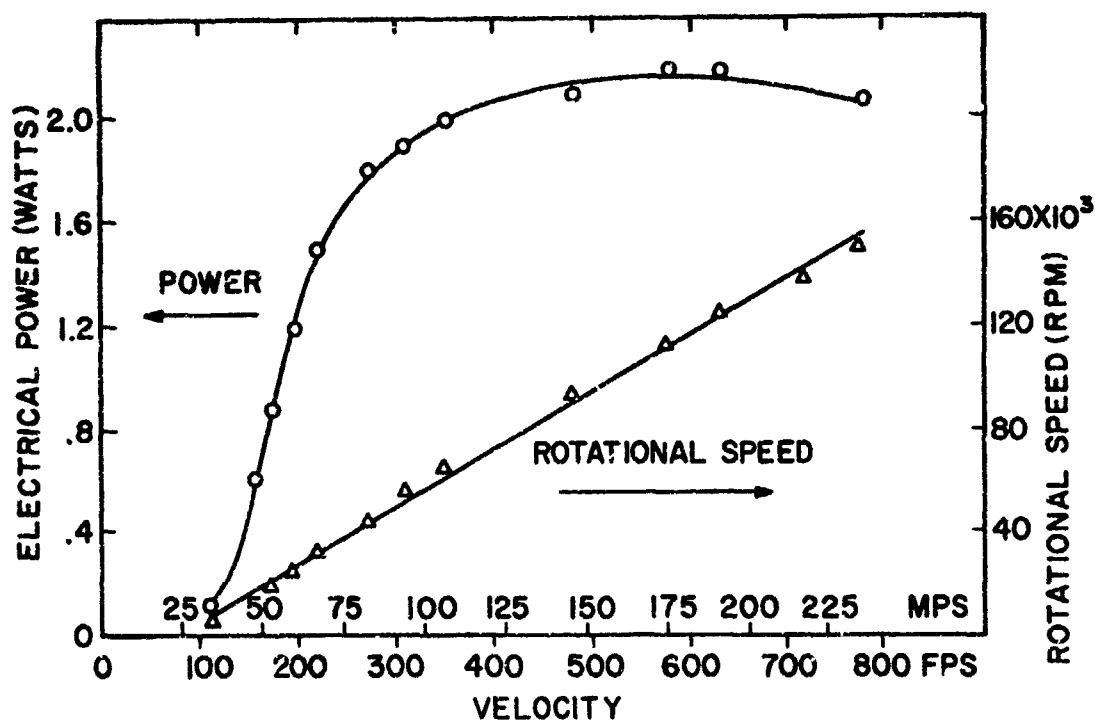


Figure 30. Electrical power output and rotational speed of 600 series alternator over 60-mm velocity range.

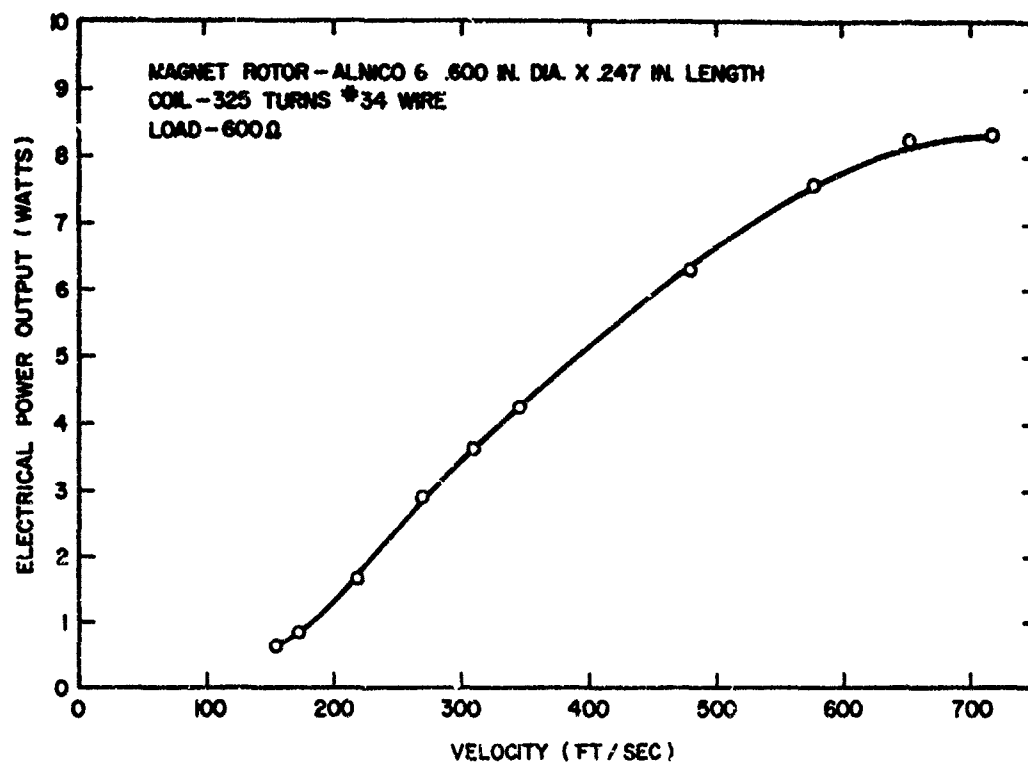


Figure 31. High-power output obtainable from 600 series casings at subsonic velocity.

increases from 0.6W at 150 ft/sec to 8.3W at 720 ft/sec (fig. 31). An alternator of this type is feasible to use in bomb fuzing applications where the operational speed is between 350 and 800 ft/sec, and power output greater than 3W is required.

8. SUMMARY AND CONCLUSIONS

An air-driven alternator was developed to provide electrical energy and drive the mechanical arming system of the 60-mm multioption fuze. Initial development of the alternator to meet the fuze requirements is described in reference 1. The alternator was subsequently tested for operating characteristics in environments of rain, temperature extremes, and in the wind tunnel.

The alternators operated without damage or observable degradation of electrical power for a combined time of 10 sec in two tests which covered a velocity range from 250 to 650 ft/sec in a rain field with intensity of 20 to 24 in./hr.

The alternators were subjected to temperature extremes ranging from -60° to $+160^{\circ}$ F. A reduction in electrical power of about 15 percent of the room temperature value occurred at $+160^{\circ}$ F over the velocity range up to 180 ft/sec. The reduced output power is still sufficient to operate the fuze (see fig. 30). The output power at -60° F was higher than that at room temperature.

Wind tunnel tests of alternator rotational speed versus velocity and angle of attack showed that:

1. At zero angle of attack, the laboratory measurements are a good indication of alternator output for the ogive shapes studied.
2. The effect of angle of attack on rotational speed depends on ogive shape, which may be evaluated under wind-tunnel conditions.
3. Of the two ogive designs tested, the one having a conical shape is less susceptible to changes in rotational speed with angle of attack.

The alternator-stator casings were redesigned to permit reproduction by a stamping process. The magnetic circuit parameters were then adjusted to meet the fuze power requirements (fig. 30). For this design (600series), the rotor is 0.600 in. diameter x 0.200 in. length. The stator pole width is 0.292 in. The wind tunnel and environmental tests that were conducted with the 500 series alternators apply also to the 600 series design, since the performance of the two devices is similar.